

Coexistence of three heteroclinic cycles and chaos analyses for a class of 3D piecewise affine systems

Fanrui Wang,¹ Zhouchao Wei,^{1,2} Wei Zhang,³ and Irene Moroz⁴

¹*School of Mathematics and Physics, China University of Geosciences, Wuhan, 430074, China*

²*Zhejiang Institute, China University of Geosciences, Hangzhou, Zhejiang 311305, China*

³*College of Mechanical Engineering, Beijing University of Technology, Beijing 100124, China*

⁴*Mathematical Institute, University of Oxford, Oxford OX2 6GG, England*

(*Electronic mail: weizhouchao@163.com)

(Dated: 6 January 2023)

Our objective is to investigate the innovative dynamics of piecewise smooth systems with multiple discontinuous switching manifolds. This paper establishes the coexistence of heteroclinic cycles in a class of 3D piecewise affine systems with three switching manifolds through rigorous mathematical analysis. By constructing suitable Poincaré maps adjacent to heteroclinic cycles, we demonstrate the occurrence of two distinct types of horseshoes and show the conditions for the presence of chaotic invariant sets. A family of attractors that satisfy the criteria are presented using this technique. It is shown that the outcomes of numerical simulation accurately reflect those of our theoretical results.

Shil'nikov theorem emphasizes that analyzing the existence of homoclinic orbits and heteroclinic cycles is of great significance for exploring chaotic behaviors of dynamic systems. In recent years, great progress has been made in the study of singular cycles for piecewise affine systems with single or two switching manifolds. Nevertheless, the pertinent research on the case of multiple switching manifolds is less, but it is indeed worthwhile since more varieties of singular cycles and chaotic invariant sets can coexist in this scenario. For this purpose, we expand the study of a class of 3D piecewise affine systems with three switching manifolds, and demonstrate the coexistence of heteroclinic cycles in addition to the coexistence of homoclinic orbits and heteroclinic cycles. Furthermore, we establish the conditions to ensure the existence of chaotic invariant sets. A thorough description of the construction of Poincaré maps has been carried out in order to better comprehend how chaotic dynamic behaviors are produced.

global connections in a system forces, in suitable conditions, the presence of chaos in the system and in close systems.^{12–16} Shil'nikov's method is to establish the conditions that small perturbations on homoclinic orbit or heteroclinic cycle defined near hyperbolic equilibria lead to Smale horseshoe chaos in the Shil'nikov sense.^{17,18} The mechanism allows us only need to discover the conditions with regard to the construction of homoclinic orbit or heteroclinic cycle.

Analytical criteria are required to be provided in order to ensure that the motions switch from one domain to another and demonstrate the presence of singular cycles in piecewise dynamical systems.^{19–23} Since the stable and unstable manifolds for piecewise affine systems can be analytically determined, it will be convenient to seek the existence of homoclinic orbits or heteroclinic cycles. To the best of our knowledge, despite the fact that the derived discriminant conditions are frequently complicated, certain accomplishments have been produced based on the main idea of Shil'nikov theorem.

For 3D piecewise affine systems with a singular switching manifold, Wu and Yang²⁴ proved the existence of homoclinic orbits analytically. Further, Wang et al. studied the homoclinic and heteroclinic bifurcations, and obtained sufficient conditions for the birth of a periodic orbit.^{25–27} As for 3D piecewise affine systems with two switching manifolds, the requirements for the existence of two different types of heteroclinic cycles were stated by Chen et al.: the first one transversely crosses three zones, whereas the second one is made up of two heteroclinic cycles that cross two zones.²⁸ Later, Lu et al. undertook substantial study on the mathematical criterion of the existence of homoclinic orbits, heteroclinic cycles as well as chaotic invariant sets, with a focus on 3D piecewise three-zone affine systems with various types of equilibrium points.^{29–33}

Some rich chaotic behaviors have also been discovered from both analytical and numerical perspectives for the 4D piecewise affine systems with a singular switching manifold. Huan et al. provided some sufficient conditions for the existence of a chaotic invariant set for 4D piecewise linear dynamical systems with a homoclinic orbit.³⁴ After that, Wu et

I. INTRODUCTION

The design and implementation of chaos have a strong practical application background, particularly in the fields of security communication, neural network, fluid dynamics, power system, and other similar fields.^{1–3} It is challenging to identify chaotic attractors and create chaos generators due to the lack of analytical methods.^{4–6} Relying on the computer to give assisted verification, Glendinning showed that the existence of an approximate sliding homoclinic orbit, and conjectured the relationship between chaotic attractors with boundary equilibrium bifurcation.⁷ Combining the geometric feature of each linear eigenspace, a simpler construction algorithm is presented to obtain the required singular cycles.⁸ Suppose the equilibrium points are located on the opposite side, Wei et al. studied periodic orbits and chaos for 3D piecewise linear systems with two virtual stable node-foci numerically.⁹

From celebrated works by Shil'nikov and their extensions given by Tresser,^{10,11} we know that the existence of some

al.^{35,36} presented a mathematical method to show that countable infinite chaotic invariant sets exist in the neighborhood of bifocal heteroclinic cycles under some eigenvalue conditions. Meanwhile, Yang and Lu established general conditions of the existence of homoclinic orbit connecting saddle-foci, and gave a numerical result to verify the correctness of chaos analysis.³⁷

Up to now, there are some meaningful results in terms of piecewise linear dynamical systems with one or two switching manifolds. However, litter literature concerns systems with multiple switching manifolds, this sparked the author's curiosity about finding the relevant rich chaotic phenomena. Zhu et al.³⁸ investigated a new kind of 3D piecewise linear systems with three switching manifolds, and gave sufficient conditions for the coexistence of homoclinic orbit and heteroclinic cycle. In this paper, we will not only take a step forward to reveal the coexistence of three heteroclinic cycles for Zhu's 3D piecewise affine systems, but also give rigorous proof to show the generation of chaotic invariant sets. It is true that identifying the presence of chaos in some systems within a given family is one of the core issues in the study of dynamic behaviors.

The rest of this article is organized as follows. In section II, we first introduce the 3D affine systems with multiple switching manifolds and limit the equilibria in respective domains. Further, we deduce the explicit sufficient conditions for ensuring the coexistence of three heteroclinic cycles by rigorous mathematical proof. In section III, the analytic conditions of the existence of chaotic invariant sets are presented. The phase diagrams are well drawn to show the chaotic behaviors, which validates our theoretical result. In the last section IV, we summarize the main results and make a conclusion of this paper.

II. COEXISTENCE OF HETEROCLINIC CYCLES IN 3D AFFINE SYSTEMS

A. Piecewise linear systems with multiple switching manifolds

Consider the following three-dimensional piecewise linear systems

$$\dot{x} = \begin{cases} A_1 x + b_1, & x \in S_1, \\ A_2 x + b_2, & x \in S_2, \\ A_3 x + b_3, & x \in S_3, \\ A_4 x + b_4, & x \in S_4, \end{cases} \quad (1)$$

where $x = (x, y, z)^T$ and $b_i, i = 1, 2, 3, 4$ are constant vectors. The whole space is divided into four zones $S_1 = \{x \mid c^T x \leq d_1\}$, $S_2 = \{x \mid d_1 < c^T x \leq d_2\}$, $S_3 = \{x \mid d_2 < c^T x \leq d_3\}$ and $S_4 = \{x \mid c^T x > d_3\}$ by switching manifolds $\Sigma_j = \{x \mid c^T x = d_j\}$ $j = 1, 2, 3$ with $c^T = (c_1, c_2, c_3)$ being a constant vector.

Note that the sign of eigenvalues of A_i cannot be exactly the same when heteroclinic cycles occurs. Without loss of generality, we suppose that the Jacobian matrixes of A_i are

$$J_{A_i} = P_i^{-1} A_i P_i, \quad i = 1, 2, 3, 4, \quad (2)$$

where

$$J_{A_1} = \begin{pmatrix} \alpha_{A_1} & 0 & 0 \\ 0 & \beta_{A_1} & 0 \\ 0 & 0 & \lambda_{A_1} \end{pmatrix}, \quad J_{A_2} = \begin{pmatrix} \alpha_{A_2} & -\beta_{A_2} & 0 \\ \beta_{A_2} & \alpha_{A_2} & 0 \\ 0 & 0 & \lambda_{A_2} \end{pmatrix},$$

$$J_{A_3} = \begin{pmatrix} \alpha_{A_3} & -\beta_{A_3} & 0 \\ \beta_{A_3} & \alpha_{A_3} & 0 \\ 0 & 0 & \lambda_{A_3} \end{pmatrix}, \quad J_{A_4} = \begin{pmatrix} \alpha_{A_4} & 0 & 0 \\ 0 & \beta_{A_4} & 0 \\ 0 & 0 & \lambda_{A_4} \end{pmatrix},$$

with $\alpha_{A_i} > 0, \beta_{A_i} > 0, \lambda_{A_i} < 0$ and

$$P_1 = (\zeta_1 \ \zeta_2 \ \zeta_3), \quad P_2 = (\xi_1 \ \xi_2 \ \xi_3),$$

$$P_3 = (\eta_1 \ \eta_2 \ \eta_3), \quad P_4 = (\rho_1 \ \rho_2 \ \rho_3).$$

Column vectors of generalized eigenvectors $\zeta_i, \xi_i, \eta_i, \rho_i$ are defined as

$$(\zeta_{i1}, \zeta_{i2}, \zeta_{i3})^T, (\xi_{i1}, \xi_{i2}, \xi_{i3})^T,$$

$$(\eta_{i1}, \eta_{i2}, \eta_{i3})^T, (\rho_{i1}, \rho_{i2}, \rho_{i3})^T.$$

In addition, suppose $E_i = -A_i^{-1}b_i$ be the equilibria belonging to the subdomain S_i satisfying

$$c^T E_1 < d_1, \quad d_1 < c^T E_2 < d_2, \quad d_2 < c^T E_3 < d_3, \quad c^T E_4 > d_3.$$

Denote the corresponding unstable and stable manifolds as

$$W^u(E_1) = \{E_1 + l_1 \zeta_1 + l_2 \zeta_2 \mid l_1, l_2 \in R\},$$

$$W^s(E_1) = \{E_1 + l_3 \zeta_3 \mid l_3 \in R\},$$

$$W^u(E_2) = \{E_2 + k_1 \xi_1 + k_2 \xi_2 \mid k_1, k_2 \in R\},$$

$$W^s(E_2) = \{E_2 + k_3 \xi_3 \mid k_3 \in R\},$$

$$W^u(E_3) = \{E_3 + s_1 \eta_1 + s_2 \eta_2 \mid s_1, s_2 \in R\},$$

$$W^s(E_3) = \{E_3 + s_3 \eta_3 \mid s_3 \in R\},$$

$$W^u(E_4) = \{E_4 + r_1 \rho_1 + r_2 \rho_2 \mid r_1, r_2 \in R\},$$

$$W^s(E_4) = \{E_4 + r_3 \rho_3 \mid r_3 \in R\},$$

where $W^s(E_1) \cap W^u(E_2) \cap \Sigma_1 \neq \emptyset$, $W^u(E_1) \cap W^s(E_2) \cap \Sigma_1 \neq \emptyset$, $W^s(E_2) \cap W^u(E_3) \cap \Sigma_2 \neq \emptyset$, $W^u(E_2) \cap W^s(E_3) \cap \Sigma_2 \neq \emptyset$, $W^s(E_3) \cap W^u(E_4) \cap \Sigma_3 \neq \emptyset$, and $W^u(E_3) \cap W^s(E_4) \cap \Sigma_3 \neq \emptyset$.

In order to simplify the final form of analytical solutions for this system, we choose the following initial points

$$x_1 = P_1(x_1, y_1, z_1)^T + E_1, \quad x_2 = P_2(x_2, y_2, z_2)^T + E_2,$$

$$x_3 = P_3(x_3, y_3, z_3)^T + E_3, \quad x_4 = P_4(x_4, y_4, z_4)^T + E_4.$$

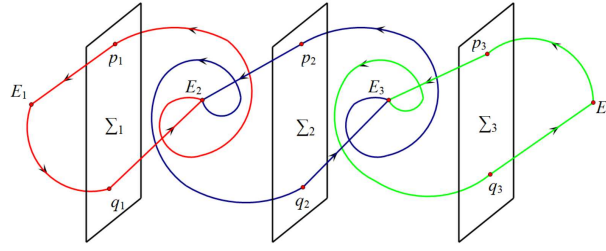


FIG. 1. Schematic diagram of the coexistence of three heteroclinic cycles Γ_1 (red lines), Γ_2 (blue lines), Γ_3 (green lines).

The obtained solutions of system (1) are given as follows

$$\begin{aligned}
 \psi_{A_1}(t, x_1) &= E_1 + e^{A_1 t}(x_1 - E_1) = E_1 + P_1 \begin{pmatrix} e^{\alpha_{A_1} t} x_1 \\ e^{\beta_{A_1} t} y_1 \\ e^{\lambda_{A_1} t} z_1 \end{pmatrix}, \\
 \psi_{A_2}(t, x_2) &= E_2 + e^{A_2 t}(x_2 - E_2) \\
 &= E_2 + P_2 \begin{pmatrix} e^{\alpha_{A_2} t}(x_2 \cos(\beta_{A_2} t) - y_2 \sin(\beta_{A_2} t)) \\ e^{\alpha_{A_2} t}(x_2 \sin(\beta_{A_2} t) + y_2 \cos(\beta_{A_2} t)) \\ e^{\lambda_{A_2} t} z_2 \end{pmatrix}, \\
 \psi_{A_3}(t, x_3) &= E_3 + e^{A_3 t}(x_3 - E_3) \\
 &= E_3 + P_3 \begin{pmatrix} e^{\alpha_{A_3} t}(x_3 \cos(\beta_{A_3} t) - y_3 \sin(\beta_{A_3} t)) \\ e^{\alpha_{A_3} t}(x_3 \sin(\beta_{A_3} t) + y_3 \cos(\beta_{A_3} t)) \\ e^{\lambda_{A_3} t} z_3 \end{pmatrix}, \\
 \psi_{A_4}(t, x_4) &= E_4 + e^{A_4 t}(x_4 - E_4) = E_4 + P_4 \begin{pmatrix} e^{\alpha_{A_4} t} x_4 \\ e^{\beta_{A_4} t} y_4 \\ e^{\lambda_{A_4} t} z_4 \end{pmatrix}.
 \end{aligned} \tag{3}$$

B. Coexistence of three heteroclinic cycles

This section focuses on providing an analytical demonstration that three heteroclinic cycles can coexist in this 3D affine system (1).

Suppose that there exist the constants $l_i, k_i, k'_i, s_i, s'_i, r_i, i = 1, 2, 3$ and points $p_1, q_1 \in \Sigma_1, p_2, q_2 \in \Sigma_2, p_3, q_3 \in \Sigma_3$ such that

$$\begin{aligned}
 p_1 &= E_1 + l_3 \zeta_3 = E_2 + k_1 \xi_1 + k_2 \xi_2, \\
 q_1 &= E_1 + l_1 \zeta_1 + l_2 \zeta_2 = E_2 + k_3 \xi_3,
 \end{aligned} \tag{4}$$

$$\begin{aligned}
 p_2 &= E_2 + k'_3 \xi_3 = E_3 + s'_1 \eta_1 + s'_2 \eta_2, \\
 q_2 &= E_2 + k'_1 \xi_1 + k'_2 \xi_2 = E_3 + s'_3 \eta_3,
 \end{aligned} \tag{5}$$

$$\begin{aligned}
 p_3 &= E_3 + s_3 \eta_3 = E_4 + r_1 \rho_1 + r_2 \rho_2, \\
 q_3 &= E_3 + s_1 \eta_1 + s_2 \eta_2 = E_4 + r_3 \rho_3.
 \end{aligned} \tag{6}$$

Theorem 1 If condition (5) hold, there exists a heteroclinic cycle Γ_2 that transversely intersects switching manifold Σ_2

and connects the equilibria E_2 and E_3 when

$$\begin{aligned}
 -\alpha_{A_2}(d_2 - c^T E_2) - \beta_{A_2}(m_{22}k'_1 - m_{21}k'_2) &< 0, \\
 -\alpha_{A_3}(d_2 - c^T E_3) - \beta_{A_3}(m_{32}s'_1 - m_{31}s'_2) &> 0, \\
 M_{22}e^{-\alpha_{A_2} T_{22}} \frac{\beta_{A_2}}{\alpha_{A_2}^2 + \beta_{A_2}^2} &< d_2 - c^T E_2, \\
 M_{22}e^{-\alpha_{A_2} T'_{22}} \frac{-\beta_{A_2}}{\alpha_{A_2}^2 + \beta_{A_2}^2} &> d_1 - c^T E_2, \\
 M_{32}e^{-\alpha_{A_2} T_{32}} \frac{\beta_{A_3}}{\alpha_{A_3}^2 + \beta_{A_3}^2} &< d_3 - c^T E_3, \\
 M_{32}e^{-\alpha_{A_2} T'_{32}} \frac{-\beta_{A_3}}{\alpha_{A_3}^2 + \beta_{A_3}^2} &> d_2 - c^T E_3,
 \end{aligned}$$

where

$$\begin{aligned}
 m_{21} &= c_1 \xi_{11} + c_2 \xi_{12} + c_3 \xi_{13}, \quad m_{22} = c_1 \xi_{21} + c_2 \xi_{22} + c_3 \xi_{23}, \\
 m_{31} &= c_1 \eta_{11} + c_2 \eta_{12} + c_3 \eta_{13}, \quad m_{32} = c_1 \eta_{21} + c_2 \eta_{22} + c_3 \eta_{23}, \\
 M_{22} &= \sqrt{(d_2 - c^T E_2)^2 + (m_{22}k'_1 - m_{21}k'_2)^2}, \\
 M_{32} &= \sqrt{(d_2 - c^T E_3)^2 + (m_{32}s'_1 - m_{31}s'_2)^2}, \\
 T_{22} &= (\pi + \arcsin \frac{d_2 - c^T E_2}{M_{22}} + \arctan \frac{\beta_{A_2}}{\alpha_{A_2}}) / \beta_{A_2}, \\
 T'_{22} &= (\arcsin \frac{d_2 - c^T E_2}{M_{22}} + \arctan \frac{\beta_{A_2}}{\alpha_{A_2}}) / \beta_{A_2}, \\
 T_{32} &= (-\arcsin \frac{d_2 - c^T E_3}{M_{32}} + \arctan \frac{\beta_{A_3}}{\alpha_{A_3}}) / \beta_{A_3}, \\
 T'_{32} &= (\pi - \arcsin \frac{d_2 - c^T E_3}{M_{32}} + \arctan \frac{\beta_{A_3}}{\alpha_{A_3}}) / \beta_{A_3}.
 \end{aligned}$$

Proof. System (1) possesses a heteroclinic cycle Γ_2 that cross the switching manifold Σ_2 transversally at p_2 and q_2 (see Fig. 1) if the following conditions hold:

- (A1) $p_2 = W^s(E_2) \cap W^u(E_3) \cap \Sigma_2, q_2 = W^u(E_2) \cap W^s(E_3) \cap \Sigma_2$;
 (A2) The positive orbit of q_2 satisfies

$$\{\psi_{A_3}(t, q_2) \mid t > 0\} \subset S_3;$$

- (A3) The negative orbit of p_2 satisfies

$$\{\psi_{A_3}(-t, p_2) \mid t > 0\} \subset S_3;$$

- (A4) The positive orbit of p_2 satisfies

$$\{\psi_{A_2}(t, p_2) \mid t > 0\} \subset S_2;$$

- (A5) The negative orbit of q_2 satisfies

$$\{\psi_{A_2}(-t, q_2) \mid t > 0\} \subset S_2;$$

- (A6) The transversality conditions

$$\begin{aligned}
 c^T(A_2 p_2 + b_2) \cdot c^T(A_3 p_2 + b_3) &> 0, \\
 c^T(A_2 q_2 + b_2) \cdot c^T(A_3 q_2 + b_3) &> 0.
 \end{aligned}$$

As we can see that condition (A1) can be directly deduced by assumption condition (5), then we can obtain that the point

$$p_2 = \begin{pmatrix} x_{E_2} + \frac{(d_2 - c^T E_2) \xi_{31}}{c_1 \xi_{31} + c_2 \xi_{32} + c_3 \xi_{33}} \\ y_{E_2} + \frac{(d_2 - c^T E_2) \xi_{32}}{c_1 \xi_{31} + c_2 \xi_{32} + c_3 \xi_{33}} \\ z_{E_2} + \frac{(d_2 - c^T E_2) \xi_{33}}{c_1 \xi_{31} + c_2 \xi_{32} + c_3 \xi_{33}} \end{pmatrix}$$

belongs to the intersection line

$$K_1 = W^u(E_3) \cap \Sigma_2 = \{E_3 + s'_1 \eta_1 + s'_2 \eta_2 \mid c_1(s'_1 \eta_{11} + s'_2 \eta_{21}) + c_2(s'_1 \eta_{12} + s'_2 \eta_{22}) + c_3(s'_1 \eta_{13} + s'_2 \eta_{23}) = d_2 - c^T E_3\},$$

and the point

$$q_2 = \begin{pmatrix} x_{E_3} + \frac{(d_2 - c^T E_3) \eta_{31}}{c_1 \eta_{31} + c_2 \eta_{32} + c_3 \eta_{33}} \\ y_{E_3} + \frac{(d_2 - c^T E_3) \eta_{32}}{c_1 \eta_{31} + c_2 \eta_{32} + c_3 \eta_{33}} \\ z_{E_3} + \frac{(d_2 - c^T E_3) \eta_{33}}{c_1 \eta_{31} + c_2 \eta_{32} + c_3 \eta_{33}} \end{pmatrix}$$

belongs to the intersection line

$$K_2 = W^u(E_2) \cap \Sigma_2 = \{E_2 + k'_1 \xi_1 + k'_2 \xi_2 \mid c_1(k'_1 \xi_{11} + k'_2 \xi_{21}) + c_2(k'_1 \xi_{12} + k'_2 \xi_{22}) + c_3(k'_1 \xi_{13} + k'_2 \xi_{23}) = d_2 - c^T E_2\}.$$

Due to the fact that $\{\psi_{A_2}(t, p_2) \mid t > 0\}$ is a line connecting p_2 and E_2 , and $\{\psi_{A_3}(t, q_2) \mid t > 0\}$ is a line connecting q_2 and E_2 , we can easy to get $\{\psi_{A_2}(t, p_2) \mid t > 0\} \subset S_2$ and $\{\psi_{A_3}(t, q_2) \mid t > 0\} \subset S_3$. Therefore, the conditions (A2) and (A4) hold.

In order to show that the condition (A3) holds, denote

$$f_1(t) = c^T(\psi_{A_3}(-t, q_2) - E_3) = M_{32} e^{-\alpha_{A_3} t} \sin(-\beta_{A_3} t + \theta_1),$$

where

$$\begin{aligned} m_{31} &= c_1 \eta_{11} + c_2 \eta_{12} + c_3 \eta_{13}, \\ m_{32} &= c_1 \eta_{21} + c_2 \eta_{22} + c_3 \eta_{23}, \\ M_{32} &= \sqrt{(d_2 - c^T E_3)^2 + (m_{32} s'_1 - m_{31} s'_2)^2}, \\ \sin \theta_2 &= \frac{d_2 - c^T E_3}{M_{32}}, \quad \cos \theta_2 = \frac{m_{32} s'_1 - m_{31} s'_2}{M_{32}}. \end{aligned}$$

Then it is equivalent to confirm that the function $f_1(t)$ is in the interval $(d_2 - c^T E_3, d_3 - c^T E_3)$.

Take the primary and secondary derivations of $f_1(t)$ with respect to the time t , we have

$$\begin{aligned} f'_1(t) &= -e^{-\alpha_{A_3} t} M_{32} [\alpha_{A_3} \sin(-\beta_{A_3} t + \theta_1) + \beta_{A_3} \cos(-\beta_{A_3} t + \theta_1)], \\ f''_1(t) &= e^{-\alpha_{A_3} t} M_{32} [(\alpha_{A_3}^2 - \beta_{A_3}^2) \sin(-\beta_{A_3} t + \theta_1) + 2\alpha_{A_3} \beta_{A_3} \cos(-\beta_{A_3} t + \theta_1)]. \end{aligned}$$

Under hypothetical conditions

$$f'_1(0) = -\alpha_{A_3} (d_2 - c^T E_3) - \beta_{A_3} (m_{32} s'_1 - m_{31} s'_2) > 0,$$

one can get $f_1(t) > d_2 - c^T E_3$ for $t \in (0, \varepsilon)$ for a sufficient small constant $\varepsilon > 0$. The corresponding damping periodic oscillating function $f_1(t)$ is shown in Fig. 2 (a).

Further, one can obtain that the equation $f'_1(t) = 0$ only when $\tan(-\beta_{A_3} t_{10} + \theta_1) = -\frac{\beta_{A_3}}{\alpha_{A_3}}$. If

$$\begin{aligned} \sin(-\beta_{A_3} t_{10} + \theta_1) &= \frac{\beta_{A_3}}{\sqrt{\alpha_{A_3}^2 + \beta_{A_3}^2}}, \\ \cos(-\beta_{A_3} t_{10} + \theta_1) &= \frac{-\alpha_{A_3}}{\sqrt{\alpha_{A_3}^2 + \beta_{A_3}^2}}, \end{aligned}$$

the quadratic derivative function $f''_1(t_{10}) < 0$, t_{10} will be the local maximum point. If

$$\begin{aligned} \sin(-\beta_{A_3} t_{10} + \theta_1) &= \frac{-\beta_{A_3}}{\sqrt{\alpha_{A_3}^2 + \beta_{A_3}^2}}, \\ \cos(-\beta_{A_3} t_{10} + \theta_1) &= \frac{\alpha_{A_3}}{\sqrt{\alpha_{A_3}^2 + \beta_{A_3}^2}}, \end{aligned}$$

the quadratic derivative function $f''_2(t_{10}) > 0$, t_{10} will be the local minimum point.

To make sure $f_1(t) \in (d_2 - c^T E_3, d_3 - c^T E_3)$ for $t \in (0, \frac{2\pi}{\beta_{A_3}})$, the maximum value and minimum value of $f_1(t)$ should satisfy

$$\begin{aligned} M_{32} e^{-\alpha_{A_3} T_{32}} \frac{\beta_{A_3}}{\alpha_{A_3}^2 + \beta_{A_3}^2} &< d_3 - c^T E_3, \\ M_{32} e^{-\alpha_{A_3} T'_{32}} \frac{-\beta_{A_3}}{\alpha_{A_3}^2 + \beta_{A_3}^2} &> d_2 - c^T E_3, \end{aligned}$$

where

$$\begin{aligned} T_{32} &= (-\arcsin \frac{d_2 - c^T E_3}{M_{32}} + \arctan \frac{\beta_{A_3}}{\alpha_{A_3}}) / \beta_{A_3}, \\ T'_{32} &= (\pi - \arcsin \frac{d_2 - c^T E_3}{M_{32}} + \arctan \frac{\beta_{A_3}}{\alpha_{A_3}}) / \beta_{A_3}. \end{aligned}$$

The process of demonstrating condition (A5) is omitted here since it can be obtained by comparing with (A3).

Finally, we establish the transversality condition (A6) as follows

$$\begin{aligned} c^T(A_3 p_2 + b_3) &= \alpha_{A_3} (d_2 - c^T E_3) + \beta_{A_3} (m_{32} s'_1 - m_{31} s'_2) < 0, \\ c^T(A_2 q_2 + b_2) &= \alpha_{A_2} (d_2 - c^T E_2) + \beta_{A_2} (m_{22} k'_1 - m_{21} k'_2) > 0, \\ c^T(A_2 p_2 + b_2) &= \lambda_{A_2} (d_2 - c^T E_2) < 0, \\ c^T(A_3 q_2 + b_3) &= \lambda_{A_3} (d_2 - c^T E_3) > 0. \end{aligned}$$

□

Theorem 2 If conditions (4) and (6) hold, there exists a heteroclinic cycle Γ_1 that transversally intersects switching manifold Σ_1 and connects the equilibria E_1 and E_2 , and exists a heteroclinic cycle Γ_3 that transversally intersects switching

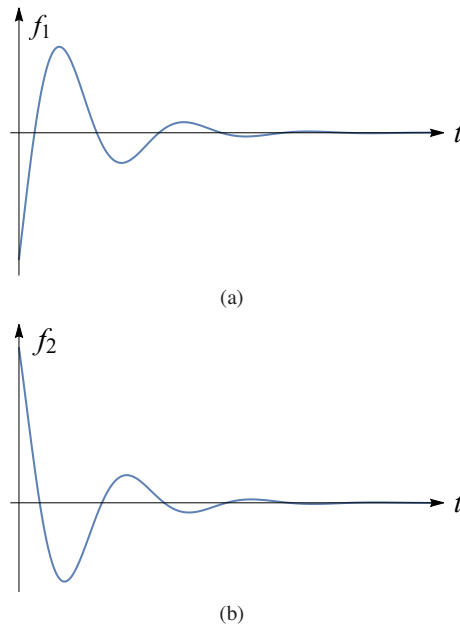


FIG. 2. The graph of (a) function $f_1(t)$ when $f_1'(0) > 0$ and (b) function $f_2(t)$ when $f_2'(0) < 0$.

manifold Σ_3 and connects the equilibria E_3 and E_4 only when

$$\begin{aligned}
 & -\alpha_{A_1} l_1 m_{11} - \beta_{A_1} l_2 m_{12} < 0, \quad -\alpha_{A_4} r_1 m_{41} - \beta_{A_4} r_2 m_{42} > 0, \\
 & -\alpha_{A_2} (d_1 - c^T E_2) - \beta_{A_2} (m_{22} k_1 - m_{21} k_2) > 0, \\
 & -\alpha_{A_3} (d_3 - c^T E_3) - \beta_{A_3} (m_{32} s_1 - m_{31} s_2) < 0, \\
 & M_{21} e^{-\alpha_{A_2} T_{21}} \frac{\beta_{A_2}}{\alpha_{A_2}^2 + \beta_{A_2}^2} < d_2 - c^T E_2, \\
 & M_{21} e^{-\alpha_{A_2} T_{21}'} \frac{-\beta_{A_2}}{\alpha_{A_2}^2 + \beta_{A_2}^2} > d_1 - c^T E_2, \\
 & M_{31} e^{-\alpha_{A_3} T_{31}} \frac{\beta_{A_3}}{\alpha_{A_3}^2 + \beta_{A_3}^2} < d_3 - c^T E_3, \\
 & M_{31} e^{-\alpha_{A_3} T_{31}'} \frac{-\beta_{A_3}}{\alpha_{A_3}^2 + \beta_{A_3}^2} > d_2 - c^T E_3,
 \end{aligned}$$

where

$$\begin{aligned}
 M_{21} &= \sqrt{(d_1 - c^T E_2)^2 + (m_{22} k_1 - m_{21} k_2)^2}, \\
 M_{31} &= \sqrt{(d_3 - c^T E_3)^2 + (m_{32} s_1 - m_{31} s_2)^2}, \\
 m_{11} &= c_1 \zeta_{11} + c_2 \zeta_{12} + c_3 \zeta_{13}, \quad m_{12} = c_1 \zeta_{21} + c_2 \zeta_{22} + c_3 \zeta_{23}, \\
 m_{21} &= c_1 \xi_{11} + c_2 \xi_{12} + c_3 \xi_{13}, \quad m_{22} = c_1 \xi_{21} + c_2 \xi_{22} + c_3 \xi_{23}, \\
 m_{31} &= c_1 \eta_{11} + c_2 \eta_{12} + c_3 \eta_{13}, \quad m_{32} = c_1 \eta_{21} + c_2 \eta_{22} + c_3 \eta_{23}, \\
 m_{41} &= c_1 \rho_{11} + c_2 \rho_{12} + c_3 \rho_{13}, \quad m_{42} = c_1 \rho_{21} + c_2 \rho_{22} + c_3 \rho_{23},
 \end{aligned}$$

and

$$\begin{aligned}
 T_{21} &= (-\arcsin \frac{d_1 - c^T E_2}{M_{21}} + \arctan \frac{\beta_{A_2}}{\alpha_{A_2}}) / \beta_{A_2}, \\
 T_{21}' &= (\pi - \arcsin \frac{d_1 - c^T E_2}{M_{21}} + \arctan \frac{\beta_{A_2}}{\alpha_{A_2}}) / \beta_{A_2}, \\
 T_{31} &= (\pi + \arcsin \frac{d_3 - c^T E_3}{M_{31}} + \arctan \frac{\beta_{A_3}}{\alpha_{A_3}}) / \beta_{A_3}, \\
 T_{31}' &= (\arcsin \frac{d_3 - c^T E_3}{M_{31}} + \arctan \frac{\beta_{A_3}}{\alpha_{A_3}}) / \beta_{A_3}.
 \end{aligned}$$

Proof. The proof of the existence of heteroclinic orbit Γ_1 can be got by analogy with the proof of the existence of heteroclinic orbit Γ_3 . We will concentrate on the detailed proof of the latter.

System (1) possesses a heteroclinic cycle Γ_3 that cross the switching manifold Σ_3 at p_3 and q_3 transversally (see Fig. 1) if the following conditions hold:

(B1) $p_3 = W^s(E_3) \cap W^u(E_4) \cap \Sigma_3$, $q_3 = W^u(E_3) \cap W^s(E_4) \cap \Sigma_3$;
 (B2) The positive orbit of q_3 satisfies

$$\{\psi_{A_4}(t, q_3) \mid t > 0\} \subset S_4;$$

(B3) The negative orbit of p_3 satisfies

$$\{\psi_{A_4}(-t, p_3) \mid t > 0\} \subset S_4;$$

(B4) The positive orbit of p_3 satisfies

$$\{\psi_{A_3}(t, p_3) \mid t > 0\} \subset S_3;$$

(B5) The negative orbit of q_3 satisfies

$$\{\psi_{A_3}(-t, q_3) \mid t > 0\} \subset S_3;$$

(B6) The transversality conditions

$$\begin{aligned}
 c^T (A_3 p_3 + b_3) \cdot c^T (A_4 p_3 + b_4) &> 0, \\
 c^T (A_3 q_3 + b_3) \cdot c^T (A_4 q_3 + b_4) &> 0.
 \end{aligned}$$

Condition (B1) can be directly deduced by condition (6), we can get that the point

$$p_3 = \begin{pmatrix} x_{E_3} + \frac{(d_3 - c^T E_3) \eta_{31}}{c_1 \eta_{31} + c_2 \eta_{32} + c_3 \eta_{33}} \\ y_{E_3} + \frac{(d_3 - c^T E_3) \eta_{32}}{c_1 \eta_{31} + c_2 \eta_{32} + c_3 \eta_{33}} \\ z_{E_3} + \frac{(d_3 - c^T E_3) \eta_{33}}{c_1 \eta_{31} + c_2 \eta_{32} + c_3 \eta_{33}} \end{pmatrix}$$

belongs to the intersection line

$$\begin{aligned}
 W_1 = W^u(E_4) \cap \Sigma_3 &= \{E_4 + r_1 \rho_1 + r_2 \rho_2 \mid c_1(r_1 \rho_{11} + r_2 \rho_{21}) \\
 &+ c_2(r_1 \rho_{12} + r_2 \rho_{22}) + c_3(r_1 \rho_{13} + r_2 \rho_{23}) = d_3 - c^T E_4\},
 \end{aligned}$$

and the point

$$q_3 = \begin{pmatrix} x_{E_4} + \frac{(d_3 - c^T E_4) \rho_{31}}{c_1 \rho_{31} + c_2 \rho_{32} + c_3 \rho_{33}} \\ y_{E_4} + \frac{(d_3 - c^T E_4) \rho_{32}}{c_1 \rho_{31} + c_2 \rho_{32} + c_3 \rho_{33}} \\ z_{E_4} + \frac{(d_3 - c^T E_4) \rho_{33}}{c_1 \rho_{31} + c_2 \rho_{32} + c_3 \rho_{33}} \end{pmatrix}$$

belongs to the intersection line

$$W_2 = W^u(E_3) \cap \Sigma_3 = \{E_3 + s_1 \eta_1 + s_2 \eta_2 \mid c_1(s_1 \eta_{11} + s_2 \eta_{21}) + c_2(s_1 \eta_{12} + s_2 \eta_{22}) + c_3(s_1 \eta_{13} + s_2 \eta_{23}) = d_3 - c^T E_3\}.$$

Since $q_3 \in \Sigma_3$ is located in one-dimensional unstable manifold of E_4 , the path of $\psi_{A_4}(t, q_3)$ for $t > 0$ is a line in S_4 . It is obvious that the condition (B2) holds. Furthermore, since the path of $\{\psi_{A_3}(t, p_3) \mid t > 0\}$ is also a line in zone S_3 , one can easily show that condition (B4) holds.

In order to show that the condition (B3) makes sense, let

$$g(t) = c^T(\psi_{A_4}(-t, p_3) - E_4) = r_1 m_{41} e^{-\alpha_{A_4} t} + r_2 m_{42} e^{-\beta_{A_4} t}, \quad (7)$$

where $m_{41} = c_1 \rho_{11} + c_2 \rho_{12} + c_3 \rho_{13}$, $m_{42} = c_1 \rho_{21} + c_2 \rho_{22} + c_3 \rho_{23}$. Then it is equivalent to proof that $g(t) > d_3 - c^T E_4$ holds for $t > 0$.

Take derivation of the equation (7), we have

$$g'(t) = -\alpha_{A_4} r_1 m_{41} e^{-\alpha_{A_4} t} - \beta_{A_4} r_2 m_{42} e^{-\beta_{A_4} t} = e^{-\beta_{A_4} t} (-\alpha_{A_4} r_1 m_{41} e^{-(\alpha_{A_4} - \beta_{A_4})t} - \beta_{A_4} r_2 m_{42}).$$

Assume that $g'(0) = -\alpha_{A_4} r_1 m_{41} - \beta_{A_4} r_2 m_{42} > 0$ to make sure $g(t) > 0$ at a small range of initial time. Based on the fact that $g(0) = d_3 - c^T E_4 < 0$ and $g(t) \rightarrow 0$ for $t \rightarrow +\infty$, we can conclude that there will have at most one root for the equation $g'(t) = 0$. Combined with monotonicity, there always has $g(t) > d_3 - c^T E_4$ no matter whether $g'(t)$ has zero roots or not.

For certificate condition (B5) holds, denote

$$f_2(t) = c^T(\psi_{A_3}(-t, q_3) - E_3) = M_{31} e^{-\alpha_{A_3} t} \sin(-\beta_{A_3} t + \theta_2),$$

where

$$\begin{aligned} m_{31} &= c_1 \eta_{11} + c_2 \eta_{12} + c_3 \eta_{13}, \\ m_{32} &= c_1 \eta_{21} + c_2 \eta_{22} + c_3 \eta_{23}, \\ M_{31} &= \sqrt{(d_3 - c^T E_3)^2 + (m_{32} s_1 - m_{31} s_2)^2}, \\ \sin \theta_2 &= \frac{d_3 - c^T E_3}{M_{31}}, \cos \theta_2 = \frac{m_{32} s_1 - m_{31} s_2}{M_{31}}. \end{aligned}$$

Then it is equivalent to confirm that the function $f_2(t)$ is in the interval $(d_2 - c^T E_3, d_3 - c^T E_3)$.

Take the primary and secondary derivations of $f_2(t)$ with respect to the time t , we have

$$\begin{aligned} f_2'(t) &= -e^{-\alpha_{A_3} t} M_{31} [\alpha_{A_3} \sin(-\beta_{A_3} t + \theta_2) + \beta_{A_3} \cos(-\beta_{A_3} t + \theta_2)], \\ f_2''(t) &= e^{-\alpha_{A_3} t} M_{31} [(\alpha_{A_3}^2 - \beta_{A_3}^2) \sin(-\beta_{A_3} t + \theta_2) + 2\alpha_{A_3} \beta_{A_3} \cos(-\beta_{A_3} t + \theta_2)]. \end{aligned}$$

Suppose $f_2'(0) = -\alpha_{A_3}(d_3 - c^T E_3) - \beta_{A_3}(m_{32} s_1 - m_{31} s_2) < 0$ to meet our expectation. The corresponding damping periodic oscillating function $f_2(t)$ is shown in Fig. 2 (b).

One can further obtain that the equation $f_2'(t) = 0$ only when $\tan(-\beta_{A_3} t_{20} + \theta_2) = -\frac{\beta_{A_3}}{\alpha_{A_3}}$. If

$$\begin{aligned} \sin(-\beta_{A_3} t_{20} + \theta_2) &= \frac{\beta_{A_3}}{\sqrt{\alpha_{A_3}^2 + \beta_{A_3}^2}}, \\ \cos(-\beta_{A_3} t_{20} + \theta_2) &= \frac{-\alpha_{A_3}}{\sqrt{\alpha_{A_3}^2 + \beta_{A_3}^2}}, \end{aligned}$$

the quadratic derivative function $f_2''(t_{20}) < 0$, t_{20} will be the local maximum point. If

$$\begin{aligned} \sin(-\beta_{A_3} t_{20} + \theta_2) &= \frac{-\beta_{A_3}}{\sqrt{\alpha_{A_3}^2 + \beta_{A_3}^2}}, \\ \cos(-\beta_{A_3} t_{20} + \theta_2) &= \frac{\alpha_{A_3}}{\sqrt{\alpha_{A_3}^2 + \beta_{A_3}^2}}, \end{aligned}$$

the quadratic derivative function $f_2''(t_{20}) > 0$, t_{20} will be the local minimum point. Based on the fact that the trajectory keeps approaching the equilibrium point E_3 , one only need to consider the extremum of the outermost trajectory is inside S_3 . Consider the time t in interval $(0, \frac{2\pi}{\beta_{A_3}})$, the corresponding maximum value and the corresponding minimum value should satisfy

$$\begin{aligned} f_2(t) &= M_{31} e^{-\alpha_{A_3} T_{31}} \frac{\beta_{A_3}}{\alpha_{A_3}^2 + \beta_{A_3}^2} < d_3 - c^T E_3, \\ f_2(t) &= M_{31} e^{-\alpha_{A_3} T'_{31}} \frac{-\beta_{A_3}}{\alpha_{A_3}^2 + \beta_{A_3}^2} > d_2 - c^T E_3, \end{aligned}$$

where

$$\begin{aligned} T_{31} &= (\pi + \arcsin \frac{d_3 - c^T E_3}{M_{31}} + \arctan \frac{\beta_{A_3}}{\alpha_{A_3}}) / \beta_{A_3}, \\ T'_{31} &= (\arcsin \frac{d_3 - c^T E_3}{M_{31}} + \arctan \frac{\beta_{A_3}}{\alpha_{A_3}}) / \beta_{A_3}. \end{aligned}$$

Finally, we show that the transversality condition (B6) holds after verifying the following conditions

$$\begin{aligned} c^T(A_3 p_3 + b_3) &= \lambda_{A_3}(d_3 - c^T E_3) < 0, \\ c^T(A_4 p_3 + b_4) &= r_1 m_{41} \alpha_{A_4} + r_2 m_{42} \beta_{A_4} < 0, \\ c^T(A_3 q_3 + b_3) &= \alpha_{A_3}(d_3 - c^T E_3) + \beta_{A_3}(m_{32} s_1 - m_{31} s_2) > 0, \\ c^T(A_4 q_3 + b_4) &= \lambda_{A_4}(d_3 - c^T E_4) > 0. \end{aligned}$$

□

Consequently, it is ready to obtain conclusion about the coexistence of three heteroclinic cycles.

Theorem 3 System (1) has the coexistence of three heteroclinic cycles when all the conditions in Theorem 1 and Theorem 2 hold.

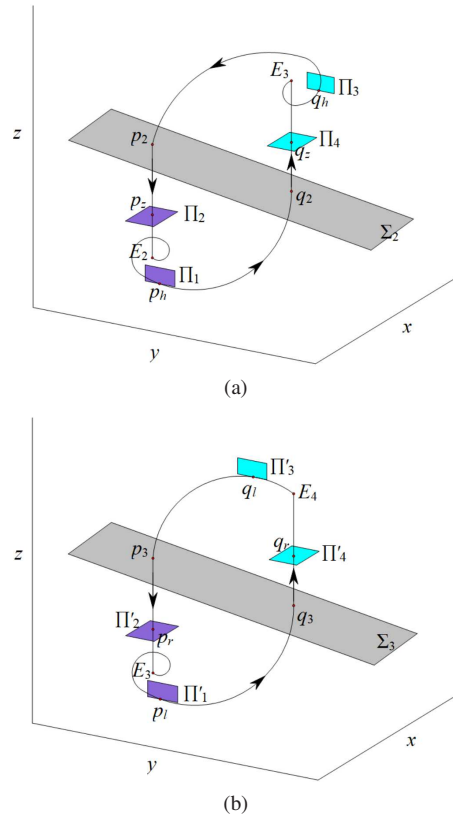


FIG. 3. Tendency and cross-sections of (a) heteroclinic cycle Γ_2 and (b) heteroclinic cycle Γ_3 .

III. THE EXISTENCE OF CHAOTIC INVARIANT SETS

Although the presence of heteroclinic cycles typically results in the production of chaotic behaviors, it remains an important yet challenging task for us to quantify this process. By structuring suitable Poincaré map, the following Theorem is established to guarantee the existence of chaotic invariant sets for system (1).

Theorem 4 Assume that heteroclinic cycles Γ_1 , Γ_2 and Γ_3 co-exist in system (1), there exhibits a chaotic invariant set Λ if one of the following conditions is satisfied

$$\begin{aligned}
 &\alpha_{A_2}\alpha_{A_3} - \lambda_{A_2}\lambda_{A_3} < 0, \\
 &\min\{\alpha_{A_1}, \beta_{A_1}\} \cdot \alpha_{A_2} - \lambda_{A_1}\lambda_{A_2} < 0, \\
 &\min\{\alpha_{A_4}, \beta_{A_4}\} \cdot \alpha_{A_3} - \lambda_{A_3}\lambda_{A_4} < 0.
 \end{aligned} \tag{8}$$

Proof. The proof will be deduced by Lemma 1 and 2 in the next subsection. \square

A. Proof of main result

To prove the existence of chaotic invariant sets, the key is to prove chaotic invariant sets are emerged from the coexistence

of heteroclinic cycles. Here, we give the diagrams about heteroclinic cycles $\Gamma_{2,3}$ and their cross-sections with switching manifolds in Fig. 3(a) and Fig. 3(b), respectively.

Lemma 1 Assume that there exists a heteroclinic cycle Γ_2 , system (1) possesses a chaotic invariant set Λ_2 if the eigenvalues of matrixes A_2 and A_3 satisfy $\alpha_{A_2}\alpha_{A_3} - \lambda_{A_2}\lambda_{A_3} < 0$.

Proof. The proof will be completed in three steps.

Step one: appropriate choice of cross sections and construct the Poincaré map. Let y_1 and y_3 be sufficiently small positive real numbers, choose the points $Z_1 = E_2 + y_1\xi_2$ and $Z_3 = E_3 + y_3\eta_2$ not located at Γ_2 but fall in the small neighborhoods of equilibria E_2 and E_3 , we obtain

$$\begin{aligned}
 Z_2 &= \psi_{A_2}\left(\frac{-2\pi}{\beta_{A_2}}, Z_1\right) = E_2 + y_2\xi_2, \\
 Z_4 &= \psi_{A_2}\left(\frac{-2\pi}{\beta_{A_3}}, Z_3\right) = E_3 + y_4\eta_2
 \end{aligned}$$

are also not located at Γ_2 where $y_2 = y_1e^{-\frac{2\pi\alpha_{A_2}}{\beta_{A_2}}}$ and $y_4 = y_3e^{-\frac{2\pi\alpha_{A_3}}{\beta_{A_3}}}$. Then it is available for us to choose cross-sections:

$$\begin{aligned}
 \Pi_1 &= \left\{ E_2 + P_2 \begin{pmatrix} 0 \\ y \\ z \end{pmatrix} \mid y_2 \leq y \leq y_1, 0 \leq z \leq \delta_1 \right\}, \\
 \Pi_2 &= \left\{ E_2 + P_2 \begin{pmatrix} x \\ y \\ \delta_2 \end{pmatrix} \mid |x| \leq \varepsilon_1, |y| \leq \varepsilon_1 \right\}, \\
 \Pi_3 &= \left\{ E_3 + P_3 \begin{pmatrix} 0 \\ y \\ z \end{pmatrix} \mid y_4 \leq y \leq y_3, 0 \leq z \leq \delta_3 \right\}, \\
 \Pi_4 &= \left\{ E_3 + P_3 \begin{pmatrix} x \\ y \\ \delta_4 \end{pmatrix} \mid |x| \leq \varepsilon_2, |y| \leq \varepsilon_2 \right\},
 \end{aligned}$$

where $\varepsilon_{1,2} > 0$, $\delta_2 > \delta_1 > 0$ and $\delta_3 > \delta_4 > 0$ being sufficiently small positive constants (see 3(a)).

Denote heteroclinic cycle Γ_2 transversality cross $\Pi_{1,2,3,4}$ at points p_h, p_z, q_h and q_z . Special selection makes it possible for $p_h = E_2 + P_2(0, y_{p_h}, 0)^T$ to be on the straight line connecting Z_1 and Z_2 , $q_h = E_3 + P_3(0, y_{q_h}, 0)^T$ to be on the straight line connecting Z_3 and Z_4 . Write

$$\Pi_1 = \bigcup_{k=0}^{\infty} R_k, \quad \Pi_3 = \bigcup_{n=0}^{\infty} \bar{R}_n,$$

where

$$R_k = \left\{ E_2 + P_2 \begin{pmatrix} x \\ y \\ z \end{pmatrix} \mid x = 0, y_2 \leq y \leq y_1, \right. \\ \left. \delta_1 e^{\frac{2(k+1)\pi\lambda_{A_2}}{\beta_{A_2}}} \leq z \leq \delta_1 e^{\frac{2k\pi\lambda_{A_2}}{\beta_{A_2}}} \right\}, \quad (9)$$

$$\bar{R}_n = \left\{ E_3 + P_3 \begin{pmatrix} x \\ y \\ z \end{pmatrix} \mid x = 0, y_4 \leq y \leq y_3, \right. \\ \left. \delta_3 e^{\frac{2(n+1)\pi\lambda_{A_3}}{\beta_{A_3}}} \leq z \leq \delta_3 e^{\frac{2n\pi\lambda_{A_3}}{\beta_{A_3}}} \right\}.$$

These selected cross-sections will make us construct six Poincaré submaps as follows

$$P_{10} : \Pi_1 \rightarrow \Sigma_2, P_{11} : \Pi_1 \rightarrow \Pi_2, P_{12} : \Pi_2 \rightarrow \Sigma_2, \\ P_{13} : \Pi_3 \rightarrow \Sigma_2, P_{14} : \Pi_3 \rightarrow \Pi_4, P_{15} : \Pi_4 \rightarrow \Sigma_2.$$

Let's begin by construct the map P_{10} . Choose an arbitrary initial point

$$X_0 = p_h + P_2(0, y, z)^T \in \Pi_1,$$

the flight time starting from X_0 to reach the switching plane Σ_2 will be the largest positive solution of the following implicit equation on t

$$F(t, y, z) = c^T (e^{A_2 t} (X_0 - E_2) + E_2) - d_2 = 0.$$

Denote t_1 as the positive flight time from p_h to q_2 , we have $F(t_1, 0, 0) = 0$ and

$$q_2 = \psi_{A_2}(t_1, p_h) = E_2 + e^{A_2 t_1} (p_h - E_2).$$

Consider the transversality of Γ_2 at q_2 in Σ_2 , we can obtain that $F'_t(t_1, 0, 0) \neq 0$. Based on the Implicit function theorem, there exists a C_1 function

$$t(y, z) = t_1 + a_1 y + a_2 z + O(2),$$

where

$$a_1 = -\frac{\frac{\partial F}{\partial y}}{\frac{\partial F}{\partial t}} \Big|_{(t,y,z)=(t_1,0,0)} = (m_{21} \sin(\beta_{A_2} t_1) - m_{22} \cos(\beta_{A_2} t_1)) / \\ (y_{p_h} ((\alpha_{A_2} m_{22} - \beta_{A_2} m_{21}) \cos(\beta_{A_2} t_1) \\ + (-\alpha_{A_2} m_{21} - \beta_{A_2} m_{22}) \sin(\beta_{A_2} t_1))),$$

$$a_2 = -\frac{\frac{\partial F}{\partial z}}{\frac{\partial F}{\partial t}} \Big|_{(t,y,z)=(t_1,0,0)} = (-m_{23} e^{(\lambda_{A_2} - \alpha_{A_2}) t_1}) / (y_{p_h} ((\alpha_{A_2} m_{22} \\ - \beta_{A_2} m_{21}) \cos(\beta_{A_2} t_1) + (-\alpha_{A_2} m_{21} - \beta_{A_2} m_{22}) \sin(\beta_{A_2} t_1))),$$

defined in a small neighborhood of p_h in Π_1 such that $F(t(y, z), y, z) \equiv 0$ holds. Taking it into the solution of subsystem (3), one can immediately get

$$\psi_{A_2}(t, X_0) = E_2 + P_2 \begin{pmatrix} -e^{\alpha_{A_2}(t_1 + a_1 y + a_2 z)} (y + y_{p_h}) \sin(\beta_{A_2}(t_1 + a_1 y + a_2 z)) \\ e^{\alpha_{A_2}(t_1 + a_1 y + a_2 z)} (y + y_{p_h}) \cos(\beta_{A_2}(t_1 + a_1 y + a_2 z)) \\ z e^{\lambda_{A_2} t_1} (1 + \lambda_{A_2} (a_1 y + a_2 z)) \end{pmatrix}.$$

Furthermore, it is available for us to obtain the submap by omitting the quadratic term of functions and truncating appropriately Taylor series expansion

$$P_{10} : \Pi_1 \rightarrow \Sigma_2, i.e. \\ p_h + P_2 \begin{pmatrix} 0 \\ y \\ z \end{pmatrix} \mapsto q_2 + P_2 \begin{pmatrix} 0 & \tau_1 & \tau_2 \\ 0 & \tau_3 & \tau_4 \\ 0 & 0 & \tau_5 \end{pmatrix} \begin{pmatrix} 0 \\ y \\ z \end{pmatrix},$$

where

$$\tau_1 = e^{\alpha_{A_2} t_1} (-\alpha_{A_2} a_1 y_{p_h} \sin(\beta_{A_2} t_1) - \beta_{A_2} a_1 y_{p_h} \cos(\beta_{A_2} t_1) \\ - \sin(\beta_{A_2} t_1)), \\ \tau_2 = e^{\alpha_{A_2} t_1} (-\alpha_{A_2} a_2 y_{p_h} \sin(\beta_{A_2} t_1) - \beta_{A_2} a_2 y_{p_h} \cos(\beta_{A_2} t_1)), \\ \tau_3 = e^{\alpha_{A_2} t_1} (\alpha_{A_2} a_1 y_{p_h} \cos(\beta_{A_2} t_1) - \beta_{A_2} a_1 y_{p_h} \sin(\beta_{A_2} t_1) \\ + \cos(\beta_{A_2} t_1)), \\ \tau_4 = e^{\alpha_{A_2} t_1} (\alpha_{A_2} a_2 y_{p_h} \cos(\beta_{A_2} t_1) - \beta_{A_2} a_2 y_{p_h} \sin(\beta_{A_2} t_1)), \\ \tau_5 = e^{\lambda_{A_2} t_1}.$$

Secondly, we present the construction the submap P_{11} . Choose an arbitrary initial point $X_1 = E_2 + P_2(0, y, z)^T$ in Π_1 , we can obtain that the flight time $t = \frac{1}{\lambda_{A_2}} \ln \frac{\delta_2}{z}$ is about the flow coming from this point to reaching the cross section Π_2 . Then it is straightforward to get the submap:

$$P_{11} : \Pi_1 \rightarrow \Pi_2, i.e. \\ E_2 + P_2 \begin{pmatrix} 0 \\ y \\ z \end{pmatrix} \mapsto E_2 + P_2 \begin{pmatrix} -y(\frac{\delta_2}{z})^{\frac{\alpha_{A_2}}{\lambda_{A_2}}} \sin(\frac{\beta_{A_2}}{\lambda_{A_2}} \ln \frac{\delta_2}{z}) \\ y(\frac{\delta_2}{z})^{\frac{\alpha_{A_2}}{\lambda_{A_2}}} \cos(\frac{\beta_{A_2}}{\lambda_{A_2}} \ln \frac{\delta_2}{z}) \\ \delta_2 \end{pmatrix}.$$

Thirdly, we construct the submap P_{12} . Choose an arbitrary initial point $X_2 = E_2 + P_2(x, y, \delta_2)^T$ in Π_2 , denote

$$G(t, x, y) = c^T (e^{A_2 t} (X_2 - E_2) + E_2) - d_2.$$

Simple calculations show that

$$G(t_2, 0, 0) = 0, G'(t_2, 0, 0) = \lambda_{A_2} (d_2 - c^T E_2) \neq 0,$$

where $t_2 = \frac{1}{\lambda_{A_2}} \ln \frac{d_2 - c^T E_2}{m_{23} \delta_2}$ is the affine time from point p_z to point p_2 . Let $r_1 = -m_{21}/m_{23}$, $r_2 = -m_{22}/m_{23}$, according to the Implicit function theorem, there exists a C_1 function

$$t(x, y) = t_2 + a_3 x + a_4 y + O(2),$$

where

$$a_3 = \frac{(r_1 \cos(\beta_{A_2} t_2) + r_2 \sin(\beta_{A_2} t_2)) e^{(\alpha_{A_2} - \lambda_{A_2}) t_2}}{\lambda_{A_2} \delta_2}, \\ a_4 = \frac{(r_1 \sin(\beta_{A_2} t_2) - r_2 \cos(\beta_{A_2} t_2)) e^{(\alpha_{A_2} - \lambda_{A_2}) t_2}}{\lambda_{A_2} \delta_2},$$

satisfying $G(t(x, y), x, y) \equiv 0$.

Substituting the affine time into the solution of subsystem (3), we can obtain

$$\psi_{A_2}(t, X_2) = E_2 + P_2 \begin{pmatrix} e^{\alpha_{A_2}(t_2+a_3x+a_4y)} (x \cos(\beta_{A_2}(t_2+a_3x+a_4y)) - y \sin(\beta_{A_2}(t_2+a_3x+a_4y))) \\ e^{\alpha_{A_2}(t_2+a_3x+a_4y)} (x \cos(\beta_{A_2}(t_2+a_3x+a_4y)) + y \sin(\beta_{A_2}(t_2+a_3x+a_4y))) \\ \delta_2 e^{\lambda_{A_2} t_2} (1 + \lambda_{A_2}(a_3x+a_4y)) \end{pmatrix}.$$

After performing Taylor series expansion retained to the first term, the following submap is constructed

$$P_{12} : \Pi_2 \rightarrow \Sigma_2, \text{ i.e. } E_2 + P_2 \begin{pmatrix} x \\ y \\ \delta_2 \end{pmatrix} \mapsto p_2 + P_2 \begin{pmatrix} o_1 & -o_2 & 0 \\ o_2 & o_1 & 0 \\ r_1 o_1 + r_2 o_2 & -r_1 o_2 + r_2 o_1 & 0 \end{pmatrix} \begin{pmatrix} x \\ y \\ 0 \end{pmatrix},$$

where $o_1 = \cos(\beta_{A_2} t_2) e^{\alpha_{A_2} t_2}$, $o_2 = \sin(\beta_{A_2} t_2) e^{\alpha_{A_2} t_2}$.

By analogy, the constructions of rest submaps can be easily found. We skip the specifics and get

$$\begin{aligned} P_{13} : \Pi_3 \rightarrow \Sigma_2, \text{ i.e. } \\ q_h + P_3 \begin{pmatrix} 0 \\ y \\ z \end{pmatrix} &\mapsto p_2 + P_3 \begin{pmatrix} 0 & \tilde{r}_1 & \tilde{r}_2 \\ 0 & \tilde{r}_3 & \tilde{r}_4 \\ 0 & 0 & \tilde{r}_5 \end{pmatrix} \begin{pmatrix} 0 \\ y \\ z \end{pmatrix}, \\ P_{14} : \Pi_3 \rightarrow \Pi_4, \text{ i.e. } \\ E_3 + P_3 \begin{pmatrix} 0 \\ y \\ z \end{pmatrix} &\mapsto E_3 + P_3 \begin{pmatrix} -y(\frac{\delta_4}{z})^{\frac{\alpha_{A_3}}{\lambda_{A_3}}} \sin(\frac{\beta_{A_3}}{\lambda_{A_3}} \ln \frac{\delta_4}{z}) \\ y(\frac{\delta_4}{z})^{\frac{\alpha_{A_3}}{\lambda_{A_3}}} \cos(\frac{\beta_{A_3}}{\lambda_{A_3}} \ln \frac{\delta_4}{z}) \\ \delta_4 \end{pmatrix}, \\ P_{15} : \Pi_4 \rightarrow \Sigma_2, \text{ i.e. } E_3 + P_3 \begin{pmatrix} x \\ y \\ \delta_4 \end{pmatrix} \\ &\mapsto q_2 + P_3 \begin{pmatrix} \tilde{o}_1 & -\tilde{o}_2 & 0 \\ \tilde{o}_2 & \tilde{o}_1 & 0 \\ \tilde{r}_1 \tilde{o}_1 + \tilde{r}_2 \tilde{o}_2 & -\tilde{r}_1 \tilde{o}_2 + \tilde{r}_2 \tilde{o}_1 & 0 \end{pmatrix} \begin{pmatrix} x \\ y \\ 0 \end{pmatrix}. \end{aligned}$$

Consequently, the whole Poincaré map is presented, that is

$$P = \bar{P}^* \circ P^* : \Pi_1 \rightarrow \Pi_1,$$

where $P^* = P_{13}^{-1} \circ P_{12} \circ P_{11}$ and $\bar{P}^* = P_{10}^{-1} \circ P_{15} \circ P_{14}$.

Step two: proving the existence of horseshoes. Denote the left boundaries of R_k and \bar{R}_n as

$$\begin{aligned} v_l &= \left\{ E_2 + P_2 \begin{pmatrix} 0 \\ y \\ z \end{pmatrix} \mid y = y_2, \delta_1 e^{\frac{2(k+1)\pi\lambda_{A_2}}{\beta_{A_2}}} \leq z \leq \delta_1 e^{\frac{2k\pi\lambda_{A_2}}{\beta_{A_2}}} \right\}, \\ \bar{v}_l &= \left\{ E_3 + P_3 \begin{pmatrix} 0 \\ y \\ z \end{pmatrix} \mid y = y_4, \delta_3 e^{\frac{2(n+1)\pi\lambda_{A_3}}{\beta_{A_3}}} \leq z \leq \delta_3 e^{\frac{2n\pi\lambda_{A_3}}{\beta_{A_3}}} \right\}. \end{aligned}$$

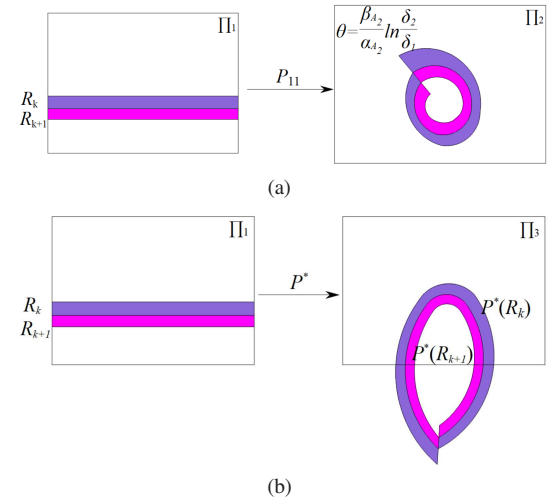


FIG. 4. The geometries of (a) R_k from Π_1 to Π_2 under the submap P_{11} , (b) R_k from Π_1 to Π_3 under the map P^* .

Polar coordinates is utilized to express the x and y components on Π_2 and Π_4 , the obtained images of boundaries v_l under map P_{11} and \bar{v}_l under map P_{14} are given by

$$\begin{aligned} P_{11}(v_l) &= \left\{ (r, \theta) \mid y_2 \left(\frac{\delta_2}{\delta_1} \right)^{\frac{\alpha_{A_2}}{\lambda_{A_2}}} e^{\frac{-2(k+1)\pi\alpha_{A_2}}{\beta_{A_2}}} \leq r \leq y_2 \left(\frac{\delta_2}{\delta_1} \right)^{\frac{\alpha_{A_2}}{\lambda_{A_2}}} e^{\frac{-2k\pi\alpha_{A_2}}{\beta_{A_2}}}, \right. \\ &\quad \left. \frac{\beta_{A_2}}{\lambda_{A_2}} \ln \frac{\delta_2}{\delta_1} - 2(k+1)\pi \leq \theta \leq \frac{\beta_{A_2}}{\lambda_{A_2}} \ln \frac{\delta_2}{\delta_1} - 2k\pi \right\}, \\ P_{14}(\bar{v}_l) &= \left\{ (r, \theta) \mid y_4 \left(\frac{\delta_4}{\delta_3} \right)^{\frac{\alpha_{A_3}}{\lambda_{A_3}}} e^{\frac{-2(n+1)\pi\alpha_{A_3}}{\beta_{A_2}}} \leq r \leq y_4 \left(\frac{\delta_4}{\delta_3} \right)^{\frac{\alpha_{A_3}}{\lambda_{A_3}}} e^{\frac{-2n\pi\alpha_{A_3}}{\beta_{A_3}}}, \right. \\ &\quad \left. \frac{\beta_{A_3}}{\lambda_{A_3}} \ln \frac{\delta_4}{\delta_3} - 2(n+1)\pi \leq \theta \leq \frac{\beta_{A_3}}{\lambda_{A_3}} \ln \frac{\delta_4}{\delta_3} - 2n\pi \right\}. \end{aligned}$$

Since the submaps of P_{10} , P_{12} , P_{13} and P_{15} are all affine submaps, the geometric structure of P^* and \bar{P}^* are similar to P_{11} and P_{14} for k sufficiently large and $\delta_{1,2,3,4}$ appropriate enough²⁹. As a comparison, Fig. 4 depicts the geometries of R_k under map P_{11} and P^* . It is evident that P_{11} continuously maps the left boundary of R_k to the internal boundary of an annulus. The internal boundary of $P^*(R_k)$ is consistent with the internal boundary of $P_{11}(R_k)$.

Subsequently, express the y, z on Π_3 by polar coordinates form. For k sufficiently large, we can obtain that there exists a positive constant L_1 such that the smallest value r_{q_h} for polar radius of the points on internal boundary near q_h satisfying

$$r_{q_h} \geq L_1 e^{\frac{-2(k+1)\pi\alpha_{A_2}}{\beta_{A_2}}}.$$

From (9), the largest value of z coordinate of upper bound-

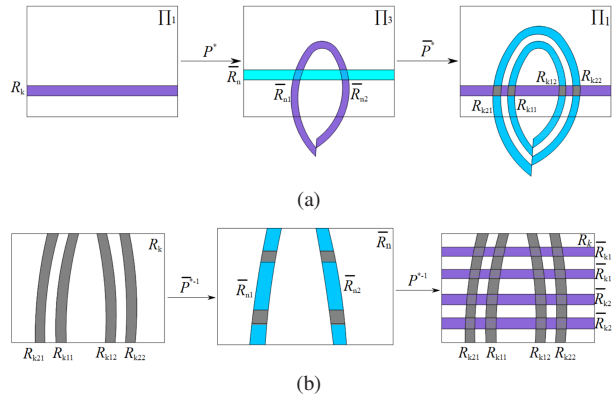


FIG. 5. (a) The geometries of \bar{R}_{ni} and R_{kij} , (b) the geometries of R_{kij} and \bar{R}_{kij} , $i, j = 1, 2$.

ary of \bar{R}_n is given by

$$(z_{\bar{R}_n})_{\max} = \delta_3 e^{\frac{2n\pi\lambda_{A_3}}{\beta_{A_3}}}.$$

Calculations reveal that there exists an integer

$$n = \left\lceil \frac{\beta_{A_3}}{2\pi\lambda_{A_3}} \ln \frac{L_1}{\delta_3} - \frac{(k+1)\alpha_{A_2}\beta_{A_3}}{\beta_{A_2}\lambda_{A_3}} \right\rceil, \quad (10)$$

which yields the inequality $r_{qh} \geq (z_{\bar{R}_n})_{\max}$ holds. This indicates that the upper boundary of \bar{R}_n will intersect with the internal boundary of $P^*(\bar{R}_k)$ at two points.

Similarly, we express the y, z on Π_1 by polar coordinates form, there will exist positive constant L_2 such that

$$r_{ph} \geq L_2 e^{-\frac{2(n+1)\pi\alpha_{A_3}}{\beta_{A_3}}}.$$

where n is given in (10).

From (9), the largest value of z coordinate of upper boundary of R_k is given by

$$(z_{R_k})_{\max} = \delta_1 e^{\frac{2k\pi\lambda_{A_2}}{\beta_{A_2}}}.$$

After a simple calculation, one can get

$$\frac{r_{ph}}{(z_{R_k})_{\max}} \geq L e^{\frac{2k\pi(\alpha_{A_2}\alpha_{A_3} - \lambda_{A_2}\lambda_{A_3})}{\beta_{A_2}\lambda_{A_3}}}$$

with $L = \frac{L_2}{\delta_1} \left(\frac{L_1}{\delta_3} \right)^{-\frac{\alpha_{A_3}}{\lambda_{A_3}}} e^{2\pi \left(\frac{\alpha_{A_2}\alpha_{A_3}}{\beta_{A_2}\lambda_{A_3}} - \frac{\alpha_{A_3}}{\beta_{A_3}} \right)}$. Moreover, we have

$$\frac{r_{ph}}{(z_{R_k})_{\max}} \rightarrow +\infty, \quad \text{if } \alpha_{A_2}\alpha_{A_3} - \lambda_{A_2}\lambda_{A_3} < 0.$$

Due to the fact that $r_{ph} \geq (z_{R_k})_{\max}$, the upper boundary of R_k will also intersect with the internal boundary of $\bar{P}^*(\bar{R}_{ni})$ at two points.

Step three: construct the horseshoe map. We have known that the intersections of $P^*(R_k)$ and \bar{R}_n are two vertical disjoint denoted by \bar{R}_{n1} and \bar{R}_{n2} . Each of them will intersect with R_k again under map \bar{P}^* , emerging two small vertical disjoint denoted by R_{ki1} and R_{ki2} . That is

$$\begin{aligned} P^*(R_k) \cap \bar{R}_n &= \bar{R}_{n1} \cup \bar{R}_{n2}, \\ \bar{P}^*(\bar{R}_{ni}) \cap R_k &= R_{ki1} \cup R_{ki2}, \quad i = 1, 2. \end{aligned}$$

The geometries of \bar{R}_{ni} and \bar{R}_{kij} for $i, j = 1, 2$ are depicted in Fig. 5(a). As is demonstrated that P^* maps the right (left) boundary of R_k to the outer (internal) boundary of $P^*(R_k)$, and \bar{P}^* maps the right (left) boundary of \bar{R}_{ni} to the outer (internal) boundary of $\bar{P}^*(\bar{R}_{ni})$.

Let \bar{R}_{ki1} and \bar{R}_{ki2} be the preimage of vertical disjoint R_{ki1} and R_{ki2} . Then P^{-1} maps the upper (lower) boundary of $\bar{R}_{k11}/\bar{R}_{k22}$ to the upper (lower) boundary of R_{k11}/R_{k22} , and maps the upper (lower) boundary of $\bar{R}_{k12}/\bar{R}_{k21}$ to the lower (upper) boundary of R_{k12}/R_{k21} . In addition, P^{-1} maps the right (left) boundary of $\bar{R}_{k11}/\bar{R}_{k22}$ to the right (left) boundary of R_{k11}/R_{k22} , and maps the right (left) boundary of $\bar{R}_{k12}/\bar{R}_{k21}$ to the left (right) boundary of R_{k12}/R_{k21} .

From the aforementioned facts, we have

$$P(\bar{R}_{kij}) = R_{kij}, \quad i, j = 1, 2.$$

The corresponding geometries of R_{kij} and \bar{R}_{kij} are shown in Fig. 5(b). By virtue of the Horseshoes lemma in piecewise continuous maps^{17,18}, if k sufficiently large, the Poincaré map P is topologically semi-conjugate to a full shift on four symbols. Thus system (1) possesses chaotic invariant sets Λ_2 . \square

Lemma 2 Assume that there exists a heteroclinic cycle Γ_1 , system (1) possesses a chaotic invariant set Λ_1 if the eigenvalues of matrixes A_1 and A_2 satisfy $\min\{\alpha_{A_1}, \beta_{A_1}\} \cdot \alpha_{A_2} - \lambda_{A_1}\lambda_{A_2} < 0$; Assume that there exists a heteroclinic cycle Γ_3 , system (1) possesses a chaotic invariant set Λ_3 if the eigenvalues of matrixes A_3 and A_4 satisfy $\min\{\alpha_{A_4}, \beta_{A_4}\} \cdot \alpha_{A_3} - \lambda_{A_3}\lambda_{A_4} < 0$.

Proof. The proof of the existence of Λ_1 and Λ_3 will be similar. For simplicity, we only prove the latter in detail.

Step one: appropriate choice of cross sections and construct the Poincaré map. First of all, select another group of desirable cross sections as follows

$$\begin{aligned} \Pi'_1 &= \left\{ E_3 + P_3 \begin{pmatrix} 0 \\ y \\ z \end{pmatrix} \mid \bar{y}_2 \leq y \leq \bar{y}_1, 0 \leq z \leq \bar{\delta}_1 \right\}, \\ \Pi'_2 &= \left\{ E_3 + P_3 \begin{pmatrix} x \\ y \\ \bar{\delta}_2 \end{pmatrix} \mid |x| \leq \bar{\epsilon}_1, |y| \leq \bar{\epsilon}_1 \right\}, \\ \Pi'_3 &= \left\{ E_4 + P_4 \begin{pmatrix} h \\ y \\ z \end{pmatrix} \mid \bar{y}_4 \leq y \leq \bar{y}_3, 0 \leq z \leq \bar{\delta}_3 \right\}, \\ \Pi'_4 &= \left\{ E_4 + P_4 \begin{pmatrix} x \\ y \\ \bar{\delta}_4 \end{pmatrix} \mid |x| \leq \bar{\epsilon}_2, |y| \leq \bar{\epsilon}_2 \right\}, \end{aligned}$$

where $\bar{\epsilon}_{1,2} > 0$, $\bar{\delta}_2 > \bar{\delta}_1 > 0$, $\bar{\delta}_3 > \bar{\delta}_4 > 0$ and h are small positive constants, and $\Pi'_1 = \bigcup_{k=0}^{\infty} H_k$ where

$$H_k = \left\{ E_3 + P_3 \begin{pmatrix} x \\ y \\ z \end{pmatrix} \middle| x = 0, \bar{y}_2 \leq y \leq \bar{y}_1, \right. \\ \left. \bar{\delta}_1 e^{\frac{2(k+1)\pi\lambda_{A_3}}{\beta_{A_3}}} \leq z \leq \bar{\delta}_1 e^{\frac{2k\pi\lambda_{A_3}}{\beta_{A_3}}} \right\}. \quad (11)$$

Denote the transversality of heteroclinic cycle Γ_3 with $\Pi'_{1,2,3,4}$ at p_l , p_r , q_l and q_r respectively (see Fig. 3(b)). Based on previous analysis, it is easy for us to construct the following submaps after some tedious calculations:

$$P_{20} : \Pi'_1 \rightarrow \Sigma_3, \text{ i.e.}$$

$$p_l + P_3 \begin{pmatrix} 0 \\ y \\ z \end{pmatrix} \mapsto q_3 + P_3 \begin{pmatrix} 0 & \gamma_1 & \gamma_2 \\ 0 & \gamma_3 & \gamma_4 \\ 0 & 0 & \gamma_5 \end{pmatrix} \begin{pmatrix} 0 \\ y \\ z \end{pmatrix},$$

$$P_{21} : \Pi'_1 \rightarrow \Pi'_2, \text{ i.e.}$$

$$E_3 + P_3 \begin{pmatrix} 0 \\ y \\ z \end{pmatrix} \mapsto E_3 + P_3 \begin{pmatrix} -y(\frac{\bar{\delta}_2}{z})^{\frac{\alpha_{A_3}}{\lambda_{A_3}}} \sin(\frac{\beta_{A_3}}{\lambda_{A_3}} \ln \frac{\bar{\delta}_2}{z}) \\ y(\frac{\bar{\delta}_2}{z})^{\frac{\alpha_{A_3}}{\lambda_{A_3}}} \cos(\frac{\beta_{A_3}}{\lambda_{A_3}} \ln \frac{\bar{\delta}_2}{z}) \\ \bar{\delta}_2 \end{pmatrix},$$

$$P_{22} : \Pi'_2 \rightarrow \Sigma_3, \text{ i.e. } E_3 + P_3 \begin{pmatrix} x \\ y \\ \bar{\delta}_2 \end{pmatrix} \\ \mapsto p_3 + P_3 \begin{pmatrix} v_1 & -v_2 & 0 \\ v_2 & v_1 & 0 \\ u_1 v_1 + u_2 v_2 & -u_1 v_2 + u_2 v_1 & 0 \end{pmatrix} \begin{pmatrix} x \\ y \\ 0 \end{pmatrix},$$

$$P_{24} : \Pi'_3 \rightarrow \Pi'_4, \text{ i.e. } E_4 + P_4 \begin{pmatrix} h \\ y \\ z \end{pmatrix} \mapsto E_4 + P_4 \begin{pmatrix} h(\frac{\bar{\delta}_4}{z})^{\frac{\alpha_{A_4}}{\lambda_{A_4}}} \\ y(\frac{\bar{\delta}_4}{z})^{\frac{\beta_{A_4}}{\lambda_{A_4}}} \\ \bar{\delta}_4 \end{pmatrix}.$$

Now, we just provide a detailed construction of P_{23} and P_{25} to prevent repetition. We first construct the map P_{23} .

Let $p_3 = E_4 + P_4(x_{p_3}, y_{p_3}, z_{p_3})^T$, $m_{43} = c_1 \rho_{31} + c_2 \rho_{32} + c_3 \rho_{33}$, the flight time of the flow from point

$$Y_0 = p_3 + P_4 \begin{pmatrix} \frac{-m_{42}y - m_{43}z}{m_{41}} \\ y \\ z \end{pmatrix} = E_4 + P_4 \begin{pmatrix} \frac{-m_{42}y - m_{43}z}{m_{41}} + x_{p_3} \\ y + y_{p_3} \\ z + z_{p_3} \end{pmatrix}$$

in Σ_3 to reaching the cross section Π'_3 is the solution of the following implicit equation on t namely

$$H(t, y, z) = c^T (e^{A_4 t} (Y_0 - E_4) + E_4) - d_3 = 0.$$

Denote t_3 as the negative flight time from p_3 to q_l . Obviously, the following formulas are satisfied

$$H(t_3, 0, 0) = 0, \quad q_l = E_4 + P_4 \begin{pmatrix} e^{\alpha_{A_4} t_3} x_{p_3} \\ e^{\beta_{A_4} t_3} y_{p_3} \\ e^{\lambda_{A_4} t_3} z_{p_3} \end{pmatrix}.$$

Moreover, we have $h = x_{p_3} e^{\alpha_{A_4} t_3}$ since $q_l \in \Pi'_3$.

Suppose that there exists $t(y, z) = t_3 + w_1 y + w_2 z + O(2)$ defined in a small neighborhood of p_3 . Taking it into the last equation of (3) and carrying out Taylor series expansion, one can get

$$\psi_{A_4}(t, Y_0) = E_4 + P_4 \begin{pmatrix} e^{\alpha_{A_4} t_3} (1 + \alpha_{A_4} (w_1 y + w_2 z)) (x_{p_3} + \frac{-m_{42}y - m_{43}z}{m_{41}}) \\ e^{\beta_{A_4} t_3} (1 + \alpha_{A_4} (w_1 y + w_2 z)) (y + y_{p_3}) \\ e^{\lambda_{A_4} t_3} (1 + \alpha_{A_4} (w_1 y + w_2 z)) (z + z_{p_3}) \end{pmatrix}.$$

Since the coordinate value in the x direction of Π_3 is fixed, it is not hard to see that

$$e^{\alpha_{A_4} t_3} (x_{p_3} + \alpha_{A_4} (w_1 y + w_2 z) x_{p_3} + \frac{-m_{42}y - m_{43}z}{m_{41}}) = h.$$

Then the coefficient of the first-order term of time is uniquely determined, that is $w_1 = \frac{m_{42}}{\alpha_{A_4} m_{41} x_{p_3}}$, $w_2 = \frac{m_{43}}{\alpha_{A_4} m_{41} x_{p_3}}$.

As such, we can construct the following submap

$$P_{23} : \Sigma_3 \rightarrow \Pi'_3, \text{ i.e.}$$

$$p_3 + P_4 \begin{pmatrix} \frac{-m_{42}y - m_{43}z}{m_{41}} \\ y \\ z \end{pmatrix} \mapsto q_l + P_4 \begin{pmatrix} 0 & 0 & 0 \\ 0 & \bar{\gamma}_1 & \bar{\gamma}_2 \\ 0 & \bar{\gamma}_3 & \bar{\gamma}_4 \end{pmatrix} \begin{pmatrix} 0 \\ y \\ z \end{pmatrix},$$

where

$$\bar{\gamma}_1 = (1 + \frac{\beta_{A_4} m_{42} y_{p_3}}{\alpha_{A_4} m_{41} x_{p_3}}) e^{\beta_{A_4} t_3}, \quad \bar{\gamma}_2 = \frac{\beta_{A_4} m_{43} y_{p_3} e^{\beta_{A_4} t_3}}{\alpha_{A_4} m_{41} x_{p_3}}, \\ \bar{\gamma}_3 = \frac{\lambda_{A_4} m_{42} z_{p_3} e^{\lambda_{A_4} t_3}}{\alpha_{A_4} m_{41} x_{p_3}}, \quad \bar{\gamma}_4 = (1 + \frac{\lambda_{A_4} m_{43} z_{p_3}}{\alpha_{A_4} m_{41} x_{p_3}}) e^{\lambda_{A_4} t_3}.$$

Next, we will construct the map P_{25} . Choose an arbitrary initial point $Y_1 = E_4 + P_4(x, y, \bar{\delta}_4)^T$ in Π'_4 and let

$$W(t, x, y) = c^T (e^{A_4 t} (Y_1 - E_4) + E_4) - d_3.$$

where the time $t_4 = \frac{1}{\lambda_{A_4}} \ln \frac{d_3 - c^T E_4}{m_{43} \bar{\delta}_4}$. Since

$$W(t_4, 0, 0) = 0, \quad W'(t_4, 0, 0) = \lambda_{A_4} (d_3 - c^T E_4) \neq 0,$$

based on the implicit function theorem, we can obtain that there exists a C_1 function

$$t(x, y) = t_4 + w_3 x + w_4 y + O(2),$$

where

$$w_3 = -\frac{m_{41}}{m_{43} \lambda_{A_4} \bar{\delta}_4} e^{(\alpha_{A_4} - \lambda_{A_4}) t_4}, \quad w_4 = -\frac{m_{42}}{m_{43} \lambda_{A_4} \bar{\delta}_4} e^{(\beta_{A_4} - \lambda_{A_4}) t_4},$$

satisfying $G(t(x, y), x, y) \equiv 0$.

Taking this time into the solution of subsystem (3), we can get

$$\psi_{A_3}(t, Y_1) = E_4 + P_4 \begin{pmatrix} x e^{\alpha_{A_4} t_4} (1 + \alpha_{A_4} (w_3 x + w_4 y)) \\ y e^{\beta_{A_4} t_4} (1 + \beta_{A_4} (w_3 x + w_4 y)) \\ \bar{\delta}_4 e^{\lambda_{A_4} t_4} (1 + \lambda_{A_4} (w_3 x + w_4 y)) \end{pmatrix}.$$

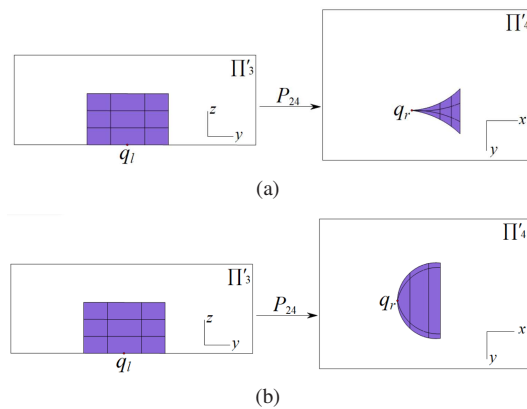


FIG. 6. Two cases of the geometry from Π'_3 to Π'_4 : (a) $\beta_{A_4} > \alpha_{A_4}$ and (b) $\alpha_{A_4} > \beta_{A_4}$.

This enables us to create the following map by extending the Taylor series expansion and retaining the primary term of coefficient functions

$$P_{25} : \Pi'_4 \rightarrow \Sigma_3, \text{ i.e.}$$

$$E_4 + P_4 \begin{pmatrix} x \\ y \\ \delta_4 \end{pmatrix} \mapsto q_3 + P_4 \begin{pmatrix} \bar{v}_1 & 0 & 0 \\ 0 & \bar{v}_2 & 0 \\ \bar{u}_1 \bar{v}_1 & \bar{u}_2 \bar{v}_2 & 0 \end{pmatrix} \begin{pmatrix} x \\ y \\ 0 \end{pmatrix},$$

where $\bar{v}_1 = e^{\alpha_{A_4} t_4}$, $\bar{v}_2 = e^{\beta_{A_4} t_4}$, $\bar{u}_1 = -\frac{m_{41}}{m_{43}}$, and $\bar{u}_2 = -\frac{m_{42}}{m_{43}}$.

Remark 1 For fully articulate how submap P_{24} influences, we take the image of a rectangle \mathcal{D} in Π'_3 as object. The submap P_{24} will map the horizontal line $z=\text{constant}$ to a line $x = h(\frac{\delta_4}{z})^{\frac{\alpha_{A_4}}{\beta_{A_4}}}$ whose length is not preserved, and will map the vertical line $y=\text{constant}$ to the tangent to x -axis (y -axis) if $\beta_{A_4} > \alpha_{A_4}$ ($\alpha_{A_4} > \beta_{A_4}$) as $z \rightarrow 0$. The $P_{24}(\mathcal{D})$ depicted in Fig. 6 shapes like a 'half-bowtie'¹⁷ or a 'bowl'²⁷. Nevertheless, the shape differences have no effect on the final associated symbolic dynamics.

Step two: proving the existence of horseshoes. Note that the submaps of P_{20}, P_{22}, P_{23} and P_{25} are all affine submaps, the geometries from Π'_1 to Π'_2 and from Π'_3 to Π'_4 are shown in Fig. 7. The geometric structure of Q^* and \bar{Q}^* are similar to P_{21} and P_{24} for k sufficiently large if we choose appropriate constants $\bar{\delta}_{1,2,3,4}$. Therefore, the Poincaré map near Γ_3 is obtained, that is

$$Q = \bar{Q}^* \circ Q^* : \Pi'_1 \rightarrow \Pi'_1,$$

where $Q^* = P_{23} \circ P_{22} \circ P_{21}$ and $\bar{Q}^* = P_{20}^{-1} \circ P_{25} \circ P_{24}$.

After making the miscellaneous but simple calculation, we demonstrate that the longitudinal length of any point on the internal boundary of $Q(H_k)$ will satisfy

$$d \geq V_1 e^{\frac{2k\pi\alpha_{A_3} \cdot \min\{\alpha_{A_4}, \beta_{A_4}\}}{\beta_{A_3}\lambda_{A_4}}},$$

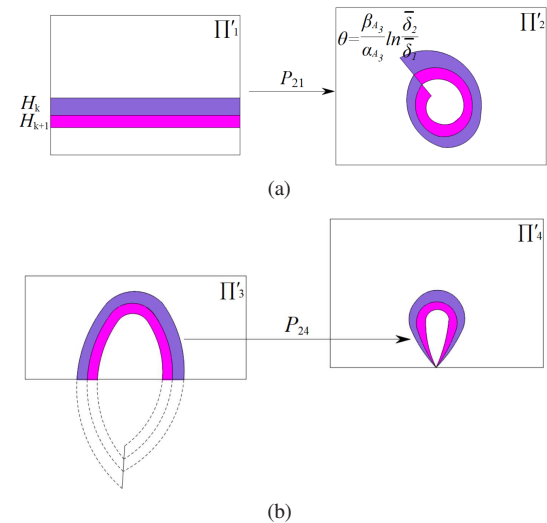


FIG. 7. The geometries (a) from Π'_1 to Π'_2 , and (b) from Π'_3 to Π'_4 .

where V_1 be a positive real number.

From the equation (11), the largest z coordinate of the upper boundary of H_k is given by

$$(z_{H_k})_{\max} = \bar{\delta}_1 e^{\frac{2k\pi\lambda_{A_3}}{\beta_{A_3}}}.$$

After a simple calculation, we can get

$$\frac{d}{(z_{H_k})_{\max}} \geq V_2 e^{\frac{2k\pi(\alpha_{A_3} \cdot \min\{\alpha_{A_4}, \beta_{A_4}\} - \lambda_{A_3}\lambda_{A_4})}{\beta_{A_3}\lambda_{A_4}}},$$

where $V_2 = \frac{V_1}{\bar{\delta}_1}$ is also a positive constant. Then we have

$$\frac{d}{(z_{H_k})_{\max}} \rightarrow +\infty, \quad \text{if } \alpha_{A_3} \cdot \min\{\alpha_{A_4}, \beta_{A_4}\} - \lambda_{A_3}\lambda_{A_4} < 0.$$

Therefore, for fixed k large enough, the upper boundary of H_k will intersect with the internal boundary of $Q(H_k)$ at two points.

Step three: construct the horseshoe map. As far as we know, under the Poincaré map Q , the previous analysis offers the following result

$$Q(H_k) \cap H_k = H_{k1} \cup H_{k2}.$$

The geometric structures of two disjoint strips H_{k1} and H_{k2} are depicted in Fig. 8(a).

Let \bar{H}_{ki} be the preimage of H_{ki} , $i = 1, 2$, the corresponding geometries of H_{ki} and \bar{H}_{ki} under the map Q^{-1} are shown in Fig. 8(b). As we can see that \bar{H}_{ki} are two disjoint horizontal strips. It is evident that Q^{-1} maps the upper (lower, left, right) boundary of H_{k1} to the upper (lower, left, right) boundary of \bar{H}_{k1} , and maps the upper (lower, left, right) boundary of H_{k2} to the lower (upper, right, left) boundary of \bar{H}_{k2} . By virtue of the Horseshoes lemma^{17,18}, we know the Poincaré map Q is topologically semi-conjugate to a full shift on two symbols if k sufficiently large.

□

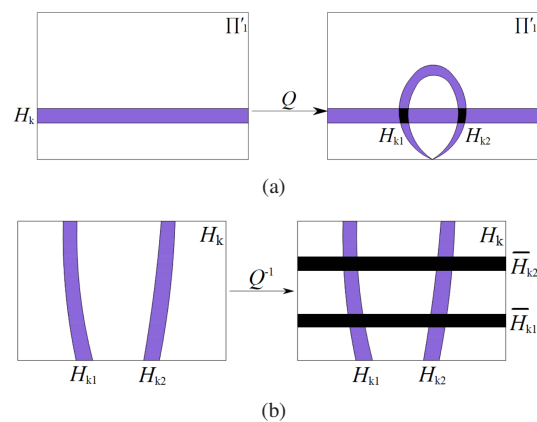


FIG. 8. The geometries of (a) H_{k1} and H_{k2} and (b) H_{ki} and \bar{H}_{ki} , $i = 1, 2$.

B. Numerical simulation

In this section, an example is given to show the coexistence of three heteroclinic cycles, and the chaotic attractor is produced by a small disturbance to the heteroclinic cycles. Consider the 3D affine system (1) where

$$A_1 = \begin{pmatrix} \frac{1}{5} & 5 & 0 \\ 0 & \frac{3}{10} & 0 \\ 0 & 0 & -15 \end{pmatrix}, A_2 = \begin{pmatrix} \frac{3}{10} & -4 & 0 \\ 4 & \frac{3}{10} & 0 \\ 0 & 0 & -10 \end{pmatrix},$$

$$A_3 = \begin{pmatrix} \frac{3}{10} & -4 & 0 \\ 4 & \frac{3}{10} & 0 \\ 0 & 0 & -10 \end{pmatrix}, A_4 = \begin{pmatrix} 1 & 0 & 0 \\ 0 & \frac{1}{20} & 0 \\ 0 & 0 & -15 \end{pmatrix},$$

$$b_1 = \begin{pmatrix} \frac{2}{25} \\ 0 \\ -6 \end{pmatrix}, b_2 = \begin{pmatrix} 0 \\ 0 \\ 0 \end{pmatrix}, b_3 = \begin{pmatrix} -\frac{3}{25} \\ -\frac{8}{5} \\ 4 \end{pmatrix}, b_4 = \begin{pmatrix} -\frac{4}{5} \\ 0 \\ 12 \end{pmatrix}.$$

Choose the specific parameter values and particular points

$$c^T = (1, 0, 1), d_1 = -\frac{2}{5}, d_2 = \frac{2}{5}, d_3 = \frac{6}{5},$$

$$l_2 = 0, l_1 = l_3 = \frac{2}{5}, k_2 = 0, k_1 = k_3 = -\frac{2}{5},$$

$$k'_2 = 0, k'_1 = k'_3 = \frac{2}{5}, s'_2 = 0, s'_1 = s'_3 = -\frac{2}{5},$$

$$s_2 = 0, s_1 = s_3 = \frac{2}{5}, r_2 = 0, r_1 = r_3 = -\frac{2}{5},$$

$$p_1 = (-\frac{2}{5}, 0, 0)^T, q_1 = (0, 0, -\frac{2}{5})^T, p_2 = (0, 0, \frac{2}{5})^T,$$

$$q_2 = (\frac{2}{5}, 0, 0)^T, p_3 = (\frac{2}{5}, 0, \frac{4}{5})^T, q_3 = (\frac{4}{5}, 0, \frac{2}{5})^T$$

satisfy all the conditions in Theorem 3 and Theorem 4. As is depicted in Fig. 9, chaotic behaviors induced by perturbing heteroclinic orbit $\Gamma_1, \Gamma_2, \Gamma_3$ are presented respectively. In addition, Fig. 10 shows the dynamic behaviors of the coexistence of heteroclinic cycles as well as the existence of chaotic invariant set Λ .

IV. CONCLUSIONS

The paper is devoted to the study of heteroclinic cycles in a class of three-dimensional piecewise affine systems with four zones of linearity. In particular, the paper provides results to ensure the coexistence of three heteroclinic cycles for this class of systems. Moreover, under the hypotheses of Theorem 3, we give a result Theorem 4 that establishes conditions for the presence of chaotic invariant set in some systems of the family by constructing Poincaré map. As a matter of fact, the main idea of Shil'nikov theorem is well-suited for the study of piecewise affine linear system, which provides a method to analytically determine the existence of chaotic invariant sets. The results of numerical simulations can well support our theoretical analysis. It is seen that the phase diagrams not only exhibit dynamic behaviors of the coexistence of heteroclinic cycles but also chaotic behaviors induced by small disturbance perturbation.

ACKNOWLEDGEMENTS

This work was supported by the National Natural Science Foundation of China (NNSFC) (Nos. 12172340, 11832002 and 11772306), Zhejiang Provincial Natural Science Foundation of China under Grant (No.LY20A020001), and the Fundamental Research Funds for the Central Universities, China University of Geosciences (CUGGC05 / CUGD-CJJ202216).

CONFLICT OF INTEREST

The authors have no conflicts to disclose.

AUTHOR CONTRIBUTIONS

Fanrui Wang: Writing – original draft (lead). Zhouchao Wei: Writing – review & editing (equal). Wei Zhang: Writing – review & editing (equal).

DATA AVAILABILITY

Data sharing is not applicable to this article as no new data were created or analyzed in this study.

REFERENCES

- ¹K. Aihara, "Chaos engineering and its application to parallel distributed processing with chaotic neural networks," *Proceedings Of The IEEE* **90**(5), 919–930 (2002).
- ²Z. C. Wei and W. Zhang, "Hidden attractors and dynamical behaviors in an extended Rikitake system," *International Journal of Bifurcation and Chaos* **24**, 1550028 (2015).

This is the author's peer reviewed, accepted manuscript. However, the online version of record will be different from this version once it has been copyedited and typeset.

PLEASE CITE THIS ARTICLE AS DOI: 10.1063/5.0132018

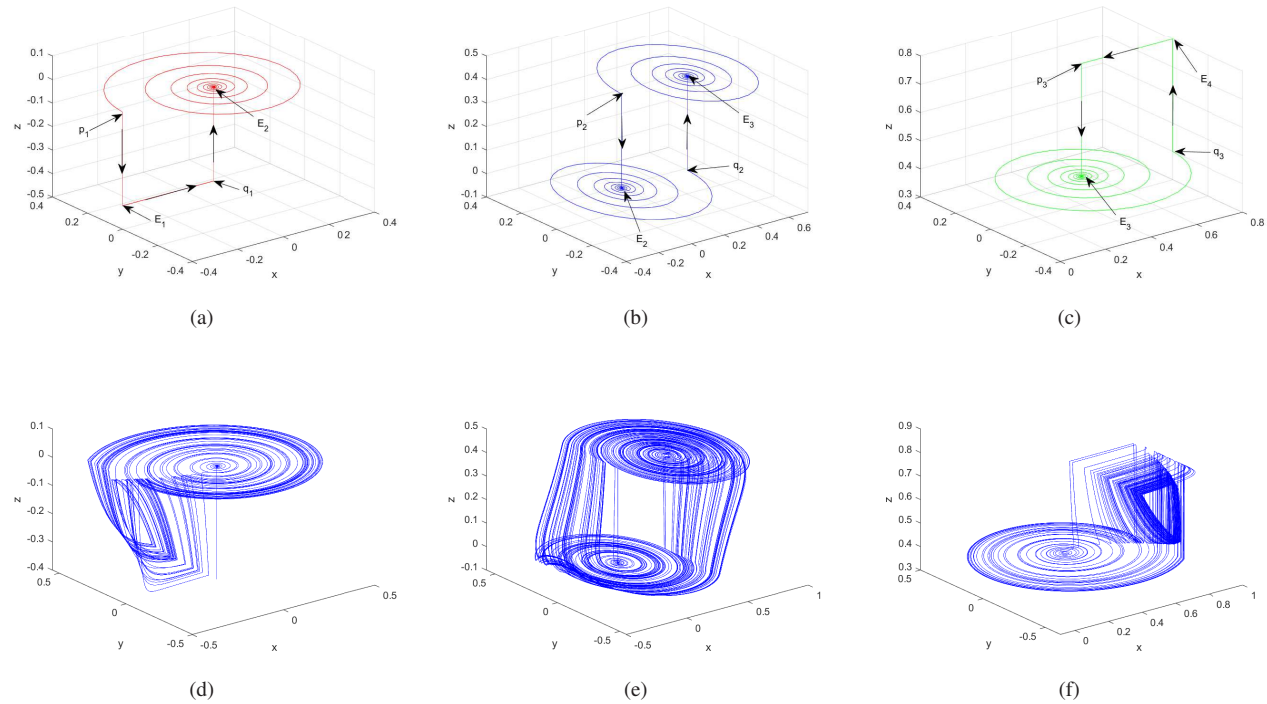


FIG. 9. (a) Heteroclinic cycle Γ_1 connecting E_1, E_2 , (b) heteroclinic cycle Γ_2 connecting E_2, E_3 , (c) heteroclinic cycle Γ_3 connecting E_3, E_4 , (d) the chaotic invariant set Λ_1 near Γ_1 , (e) the chaotic invariant set Λ_2 near Γ_2 , (f) the chaotic invariant set Λ_3 near Γ_3 .

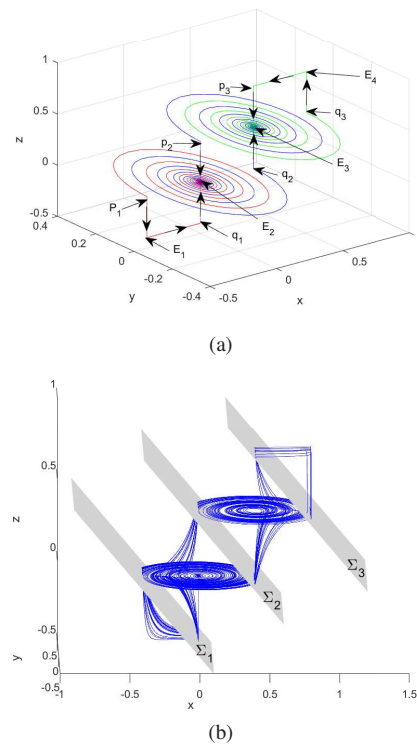


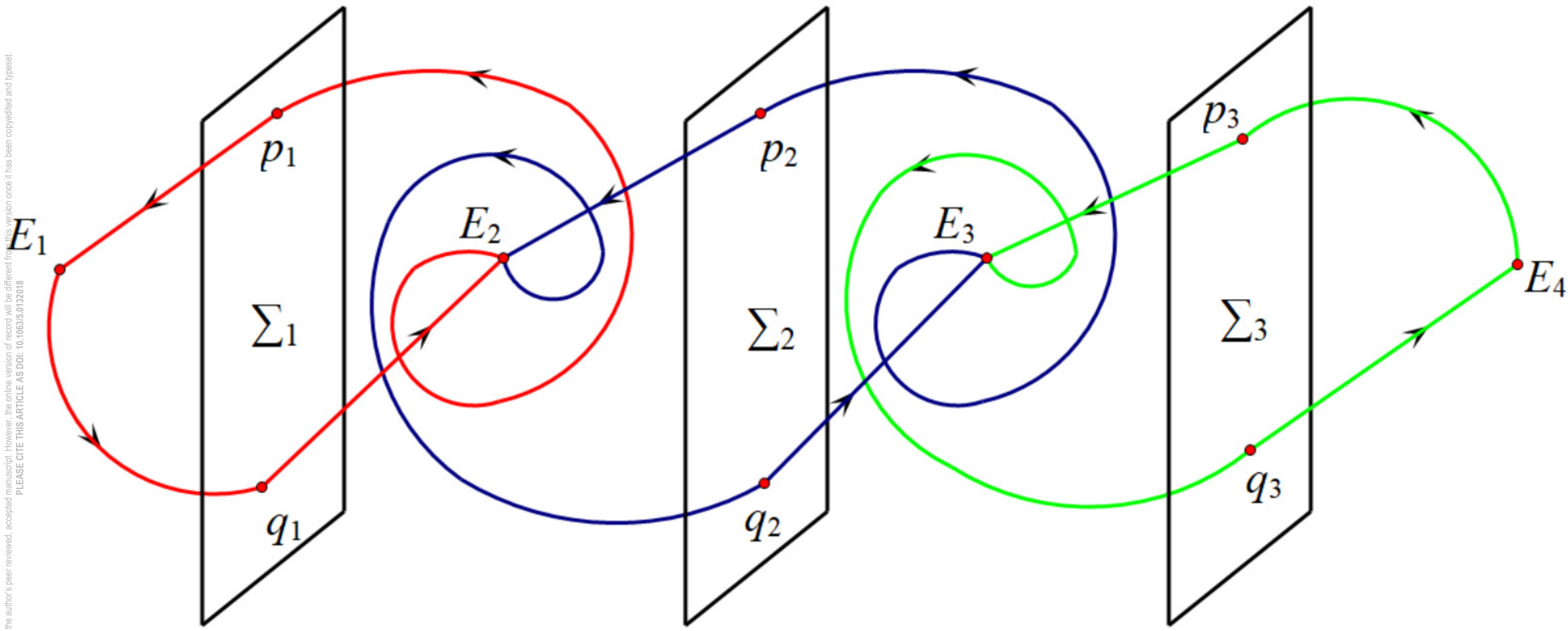
FIG. 10. (a) The coexistence of three heteroclinic cycles, and (b) the existence of chaotic invariant set Λ .

- ³J. R. Pulido-Luna, J. A. López-Rentería, N. R. Cazarez-Castro, and E. Campos, "A two-directional grid multiscroll hidden attractor based on piecewise linear system and its application in pseudo-random bit generator," *Integration, the VLSI Journal* **81**, 34–42 (2021).
- ⁴J. H. Lü, T. S. Zhou, G. R. Chen, and X. S. Yang, "Generating chaos with a switching piecewise-linear controller," *Chaos* **12**, 344–349 (2002).
- ⁵S. M. Huan, Q. D. Li, and X. S. Yang, "Chaos in three-dimensional hybrid systems and design of chaos generators," *Nonlinear Dynamics* **69**, 1915–1927 (2012).
- ⁶T. T. Wu, L. Wang, and X. S. Yang, "Chaos generator design with piecewise affine systems," *Nonlinear Dynamics* **84**(2), 817–832 (2016).
- ⁷P. A. Glendinning, "Shilnikov chaos, Filippov sliding and boundary equilibrium bifurcations," *European Journal of Applied Mathematics* **29**, 1–21 (2018).
- ⁸J. G. Barajas-Ramírez, A. Franco-López, and H. G. González-Hernández, "Generating Shilnikov chaos in 3D piecewise linear systems," *Applied Mathematics and Computation* **395**, 125877 (2021).
- ⁹Z. C. Wei, B. Zhu, and R. J. Escalante-González, "Existence of periodic orbits and chaos in a class of three-dimensional piecewise linear systems with two virtual stable node-foci," *Nonlinear Analysis: Hybrid Systems* **43**, 101114 (2021).
- ¹⁰C. P. Silva, "Shil'nikov's theorem—A tutorial," *IEEE Transactions on Circuits and Systems I: Fundamental Theory and Applications* **40**(10), 675–82 (1993).
- ¹¹C. Tresser, "About some theorems by L. P. Shil'nikov," *Annales Henri Poincaré* **40**, 440–461 (1984).
- ¹²G. A. Leonov, "Fishing principle for homoclinic and heteroclinic trajectories," *Nonlinear Dynamics* **78**(4), 2751–2758 (2014).
- ¹³S. B. Li, X. J. Gong, W. Zhang, and Y. X. Hao, "The Melnikov method for detecting chaotic dynamics in a planar hybrid piecewise-smooth system with a switching manifold," *Nonlinear Dynamics* **89**, 939–953 (2017).
- ¹⁴J. C. Sprott, "Do we need more chaos examples? Chaos," *Chaos Theory and Applications* **2**(2), 49–51 (2020).
- ¹⁵J. Ma, "Chaos theory and applications: the physical evidence, mechanism are important in chaotic systems," *Chaos Theory and Applications* **4**(1), 1–3

This is the author's peer reviewed, accepted manuscript. However, the online version of record will be different from this version once it has been copyedited and typeset.

PLEASE CITE THIS ARTICLE AS DOI: 10.1063/5.0132018

- (2022).
- ¹⁶A. Karthikeyan, M. E. Cimen, A. Akgul, A. F. Boz, and K. Rajagopal, "Persistence and coexistence of infinite attractors in a fractal Josephson junction resonator with unharmonic current phase relation considering feedback flux effect," *Nonlinear Dynamic* **103**, 1979–1998 (2021).
 - ¹⁷S. Wiggins, "Introduction to applied nonlinear dynamical systems and chaos, second edition," Springer-Verlag, New York (2003).
 - ¹⁸J. Llibre, E. Ponce, and A. E. Teruel, "Horseshoes near homoclinic orbits for piecewise linear differential systems in \mathbb{R}^3 ," *International Journal of Bifurcation and Chaos* **17**(4), 1171–1184 (2007).
 - ¹⁹A. C. J. Luo, "Discontinuous dynamical systems," Springer-Verlag, Berlin (2012).
 - ²⁰R. Cristiano, T. Carvalho, D. J. Tonon, and D. J. Pagano, "Hopf and Homoclinic bifurcations on the sliding vector field of switching systems in \mathbb{R}^3 : A case study in power electronics," *Physica D* **347**, 12–20 (2017).
 - ²¹H. A. Hosham, "Nonlinear behavior of a novel switching Jerk system," *International Journal of Bifurcation and Chaos* **30**, 2050202 (2020).
 - ²²V. N. Belykh, N. V. Barabash, and I. V. Belykh, "Sliding homoclinic bifurcations in a Lorenz-type system: Analytic proofs," *Chaos* **31**, 043117 (2021).
 - ²³Z. T. Njitacke, T. F. Fozin, L. K. Kamdjeu, G. D. Leutcho, E. M. Kengne and J. Kengne, "Multistability and its annihilation in the Chua's oscillator with piecewise-linear nonlinearity," *Chaos Theory and Applications* **2**(2), 77–89 (2020).
 - ²⁴T. T. Wu and X. S. Yang, "A new class of 3-dimensional piecewise affine systems with homoclinic orbits," *Discrete and Continuous Dynamical Systems* **36**(9), 5119–5129 (2016).
 - ²⁵L. Wang and X. S. Yang, "Existence of homoclinic cycles and periodic orbits in a class of three-dimensional piecewise affine systems," *International Journal of Bifurcation and Chaos* **28**, 1850024 (2018).
 - ²⁶L. Wang, Q. D. Li, and X. S. Yang, "Periodic sinks and periodic saddle orbits induced by heteroclinic bifurcation in three-dimensional piecewise linear systems with two zones," *Applied Mathematics and Computation* **404**, 126200 (2021).
 - ²⁷L. Wang and X. S. Yang, "Heteroclinic cycles in a class of 3-dimensional piecewise affine systems," *Nonlinear Analysis: Hybrid Systems* **23**, 44–60 (2017).
 - ²⁸Y. L. Chen, L. Wang, and X. S. Yang, "On the existence of heteroclinic cycles in some class of 3-dimensional piecewise affine systems with two switching planes," *Nonlinear Dynamics* **91**, 67–79 (2018).
 - ²⁹K. Lu, Q. G. Yang, and W. J. Xu, "Heteroclinic cycles and chaos in a class of 3D three-zone piecewise affine systems," *Journal of Mathematical Analysis and Applications* **478**, 58–81 (2019).
 - ³⁰K. Lu, Q. G. Yang, and G. R. Chen, "Singular cycles and chaos in a new class of 3D three-zone piecewise affine systems," *Chaos* **29**(4), 043124 (2019).
 - ³¹K. Lu, W. J. Xu, and Q. M. Xiang, "Coexistence of singular cycles in a new kind of 3D non-smooth systems with two discontinuous boundaries," *Nonlinear Dynamics* **104**, 149–164 (2021).
 - ³²K. Lu and W. J. Xu, "Coexisting singular cycles in a class of three-dimensional three-zone piecewise affine systems," *Discrete and Continuous Dynamical Systems–Series B* **27**, 7315–7349 (2022).
 - ³³K. Lu, W. J. Xu, Y. C. Wei, and W. Xu, "Heteroclinic cycles generated by piecewise affine systems in \mathbb{R}^n ," *International Journal of Bifurcation and Chaos* **32**, 2250146 (2022).
 - ³⁴S. M. Huan and X. S. Yang, "Existence of chaotic invariant set in a class of 4-dimensional piecewise linear dynamical systems," *International Journal of Bifurcation and Chaos* **24**, 1450158 (2014).
 - ³⁵T. T. Wu and X. S. Yang, "On the existence of bifocal heteroclinic cycles in a class of four-dimensional piecewise affine systems," *Chaos* **26**, 053104 (2016).
 - ³⁶T. T. Wu, L. Wang, and X. S. Yang, "Chaotic dynamics in four-dimensional piecewise affine systems with bifocal heteroclinic cycles," *International Journal of Bifurcation and Chaos* **28**(11), 1850141 (2018).
 - ³⁷Q. G. Yang and K. Lu, "Homoclinic orbits and an invariant chaotic set in a new 4D piecewise affine systems," *Nonlinear Dynamics* **93**, 2445–2459 (2018).
 - ³⁸B. Zhu, Z. C. Wei, R. J. Escalante-González, and N. V. Kuznetsov, "Existence of homoclinic orbits and heteroclinic cycle in a class of three-dimensional piecewise linear systems with three switching manifolds," *Chaos* **30**, 123143 (2020).





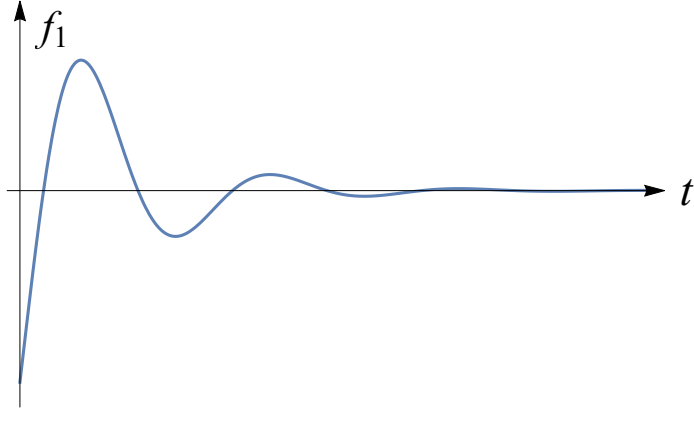
**AIP
Publishing**

Chaos

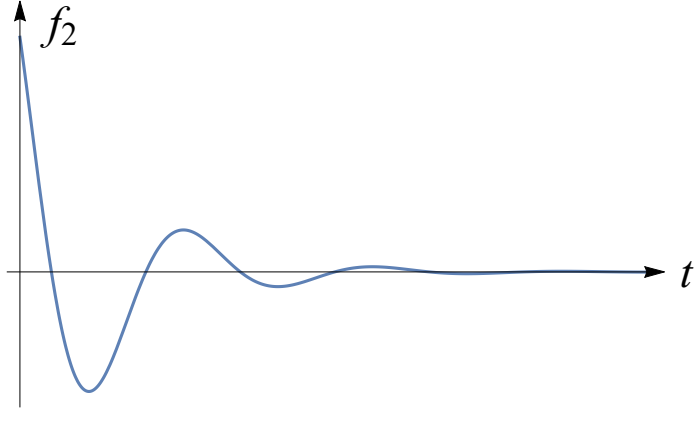
An Interdisciplinary Journal
of Nonlinear Science

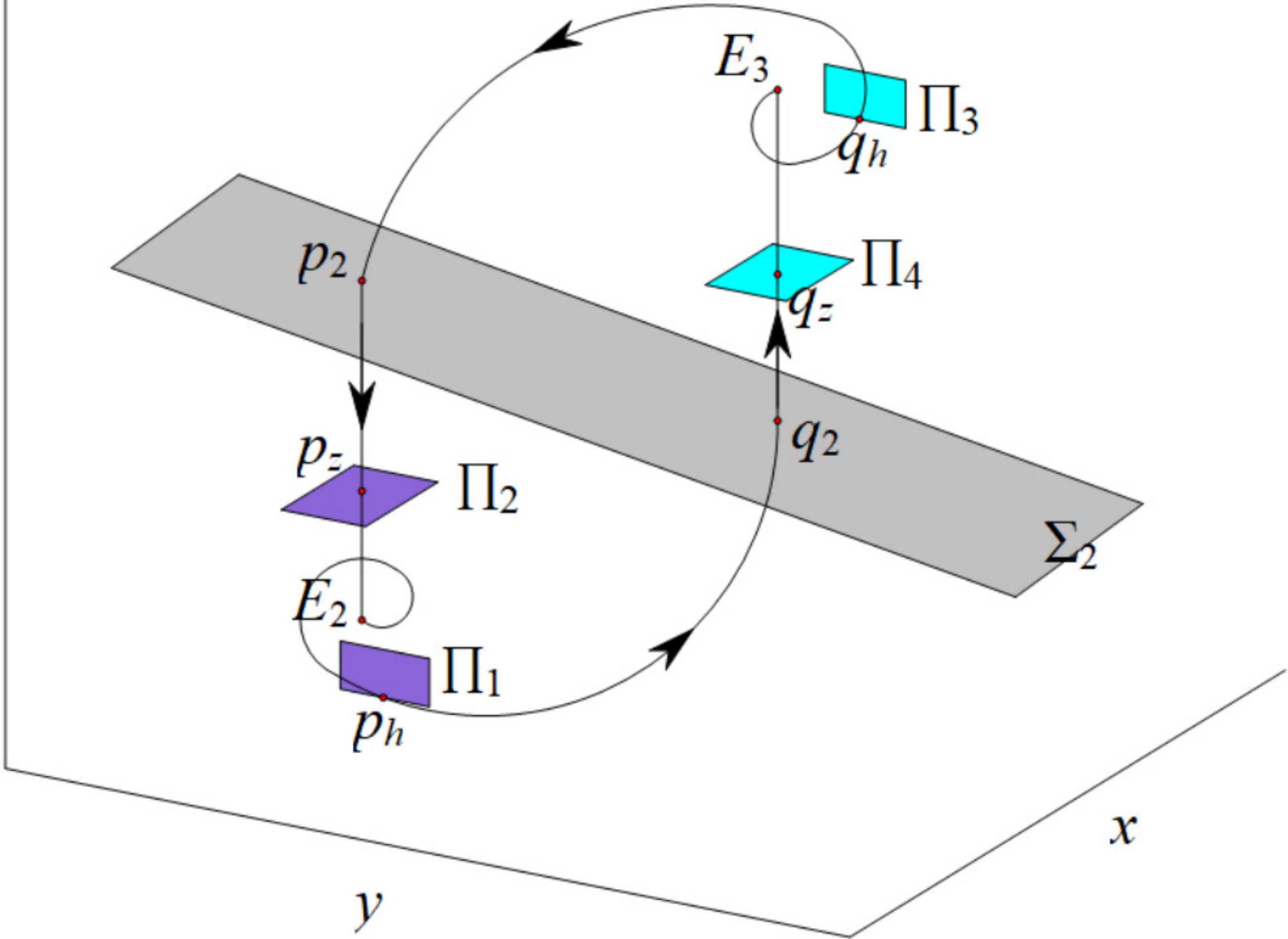
ACCEPTED MANUSCRIPT

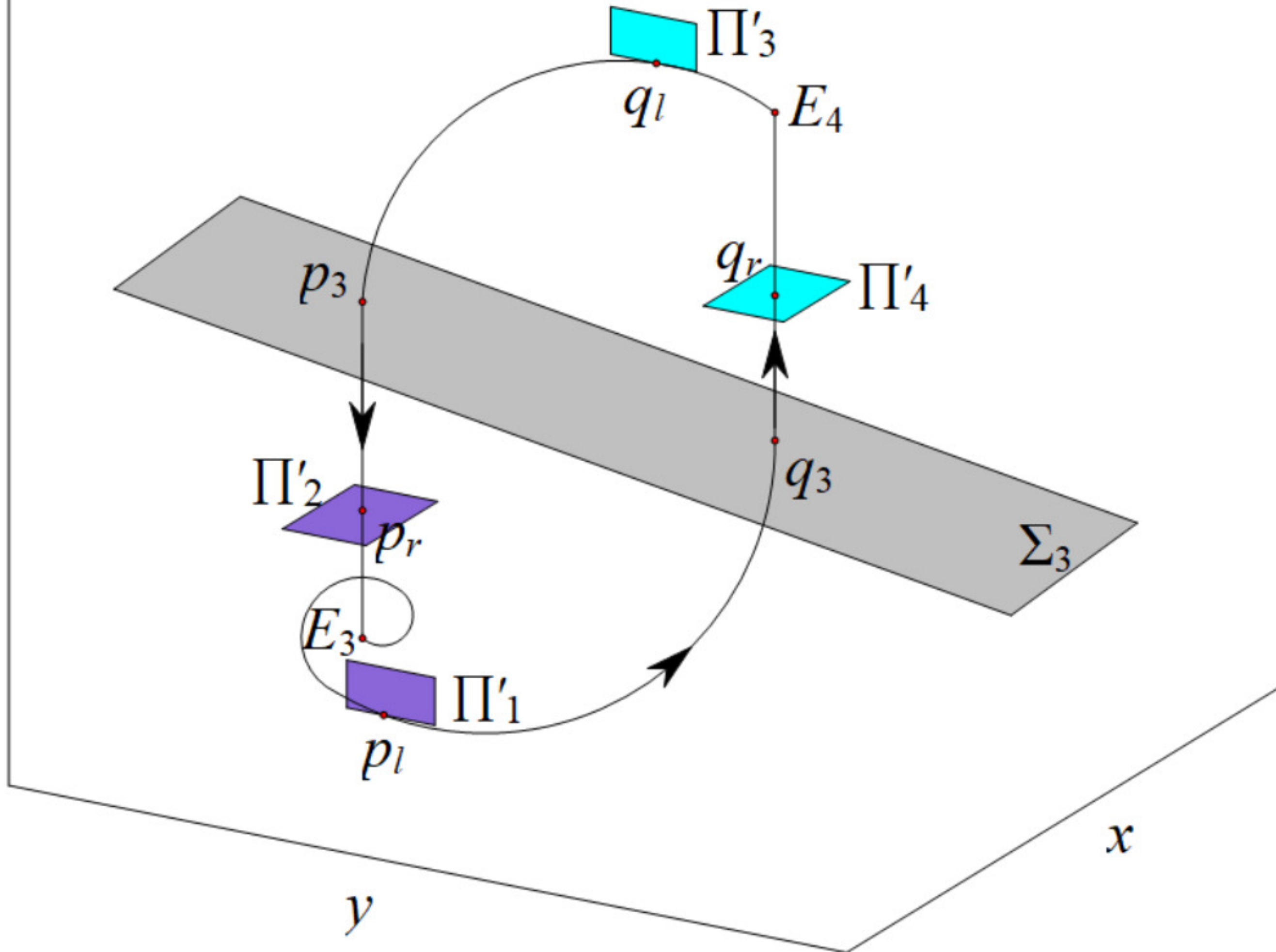
This is the author's peer reviewed, accepted manuscript. However, the online version of record will be different from this version once it has been copyedited and typeset.
PLEASE CITE THIS ARTICLE AS DOI: 10.1063/5.0132018



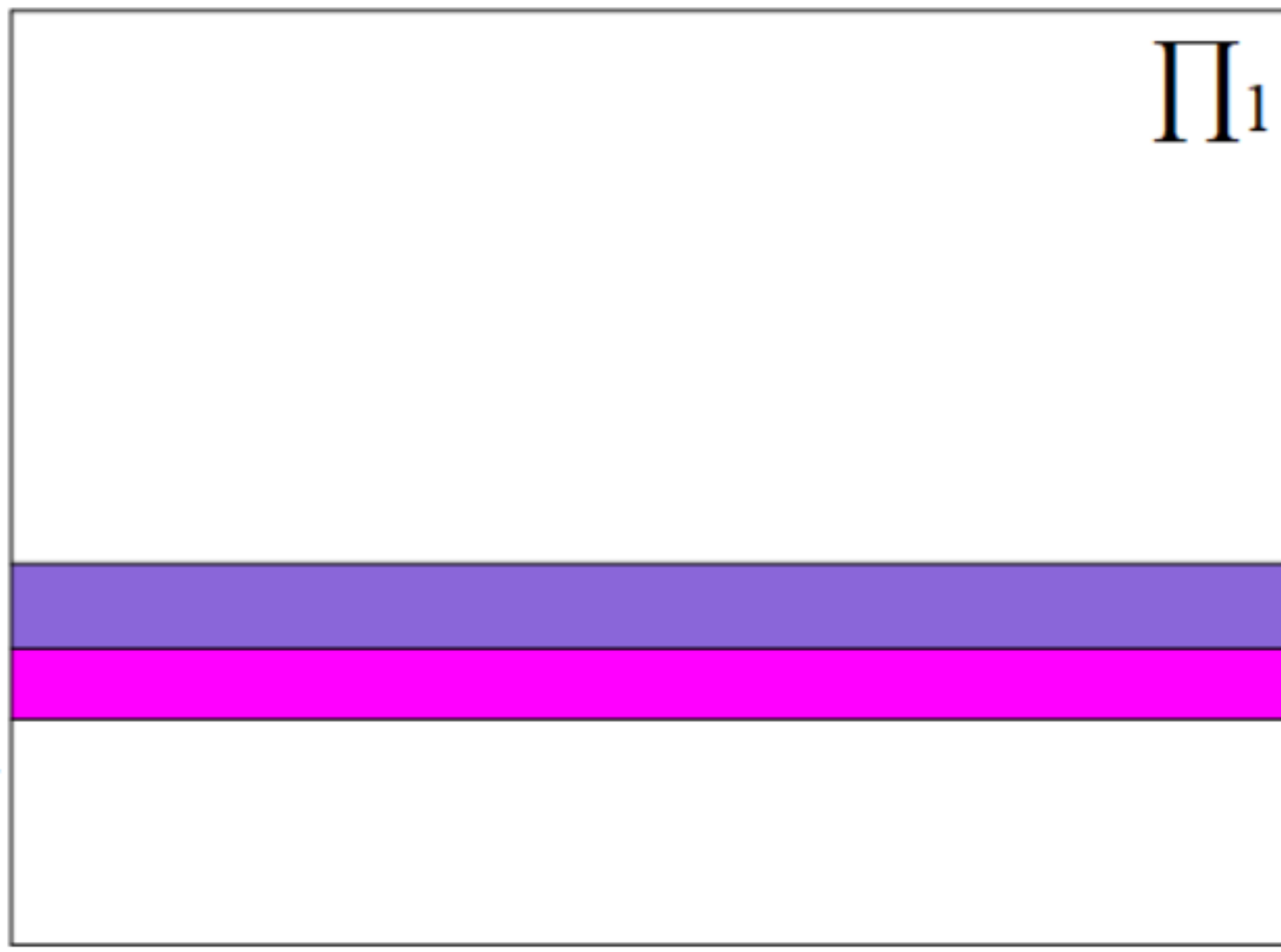
This is the author's peer reviewed, accepted manuscript. However, the online version of record will be different from this version once it has been copyedited and typeset.
PLEASE CITE THIS ARTICLE AS DOI: 10.1063/5.0132018



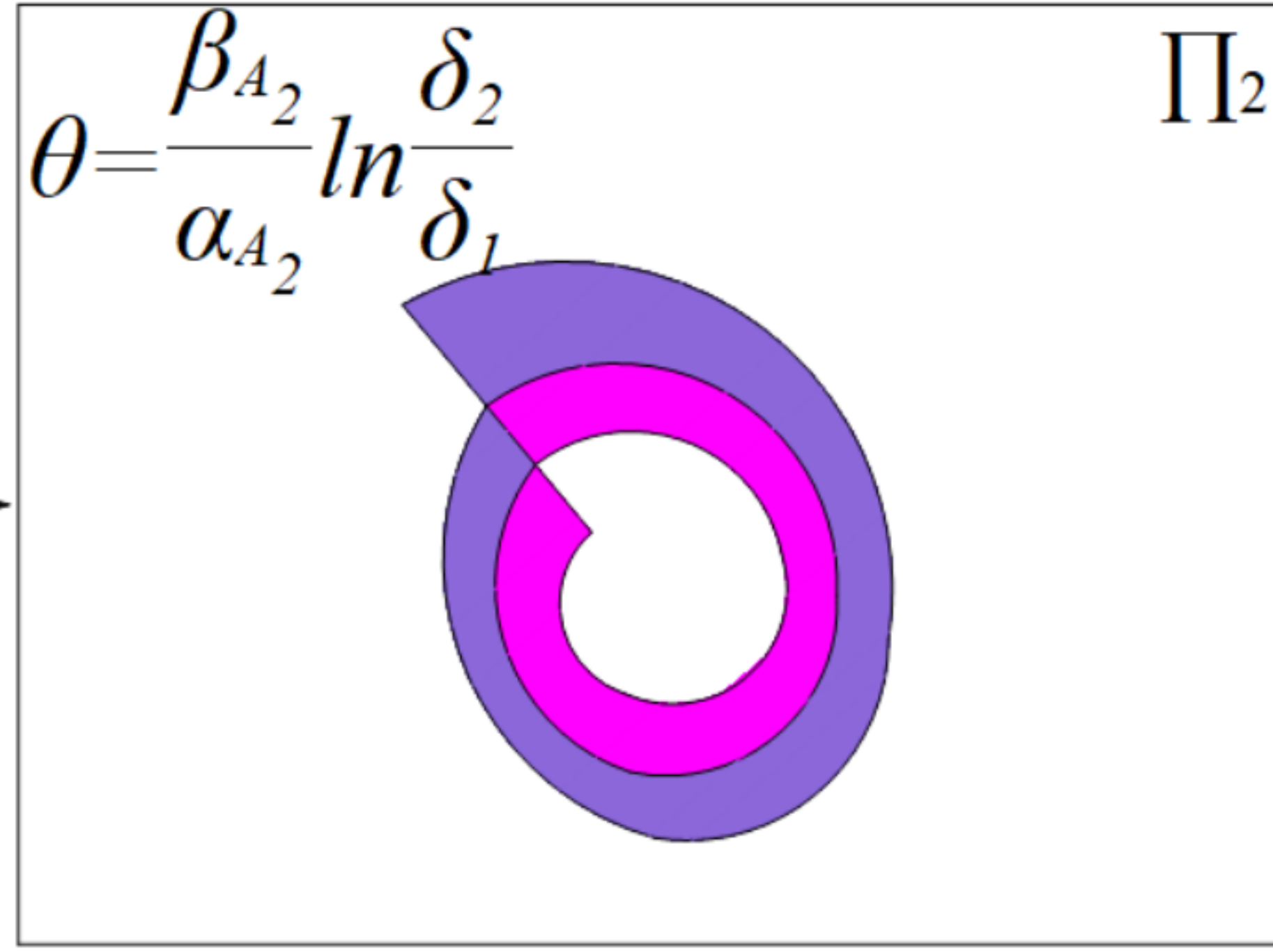


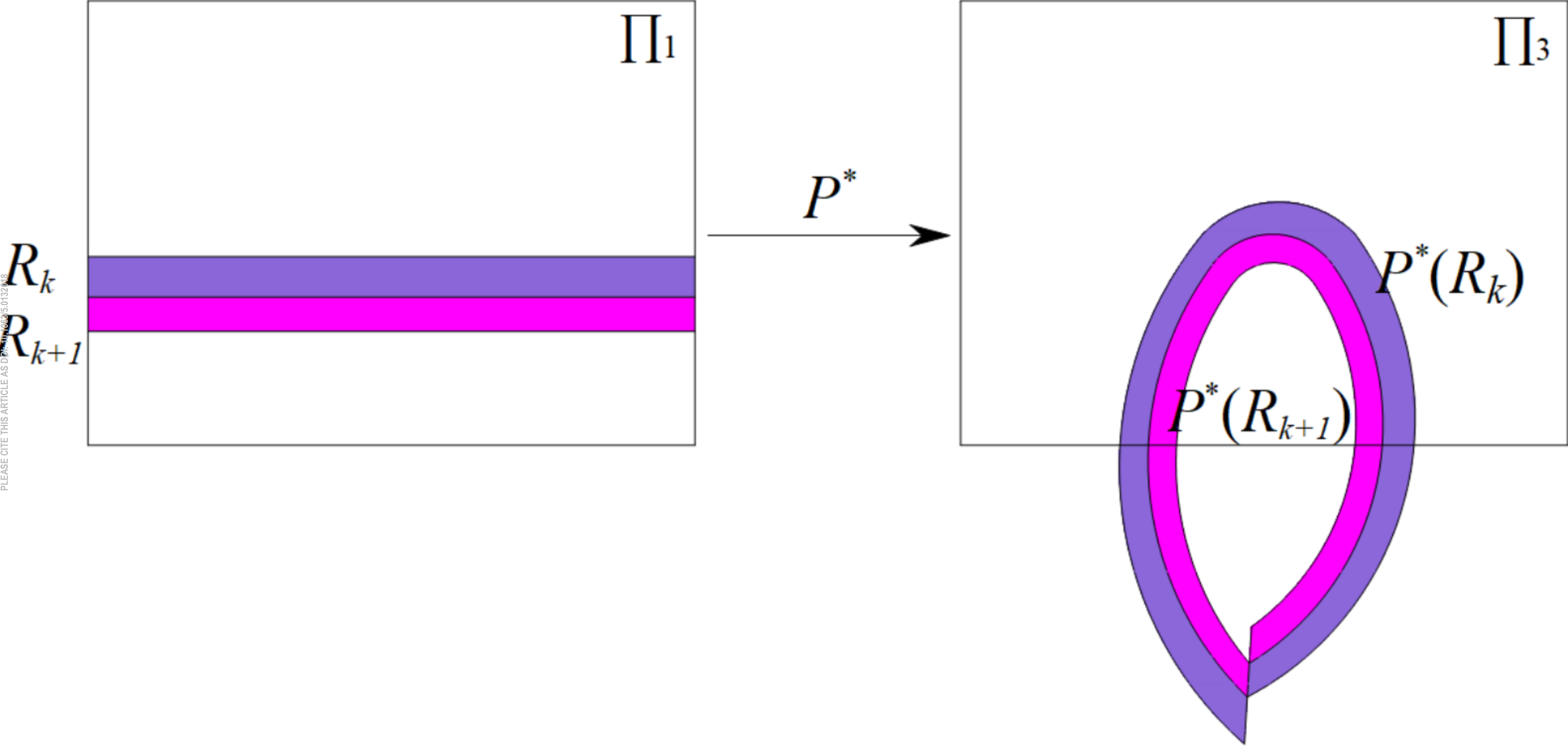


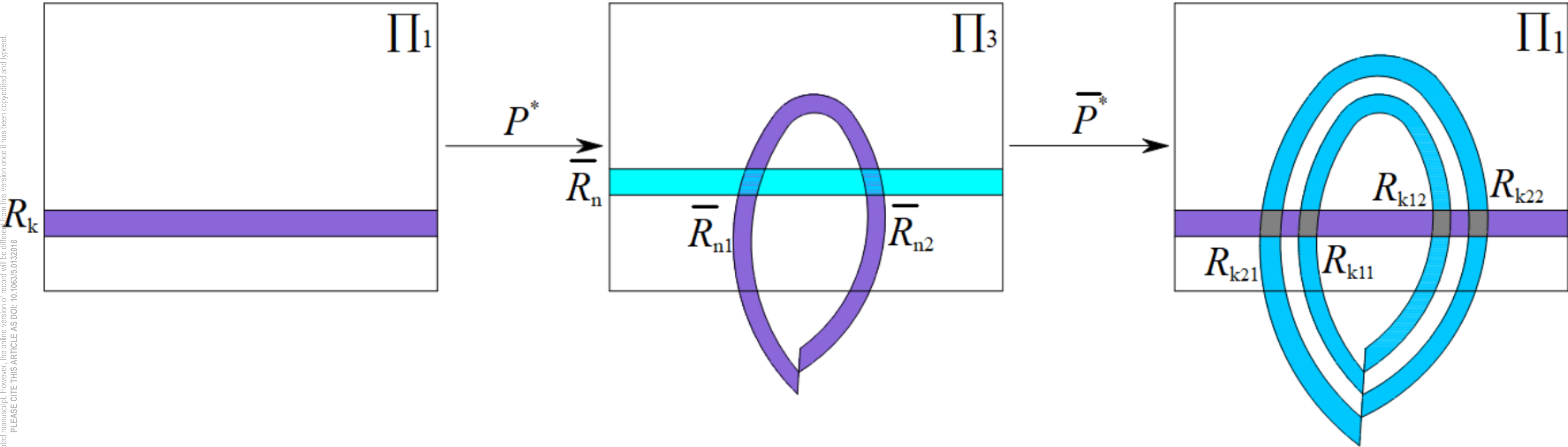
R_k
 R_{k+1}

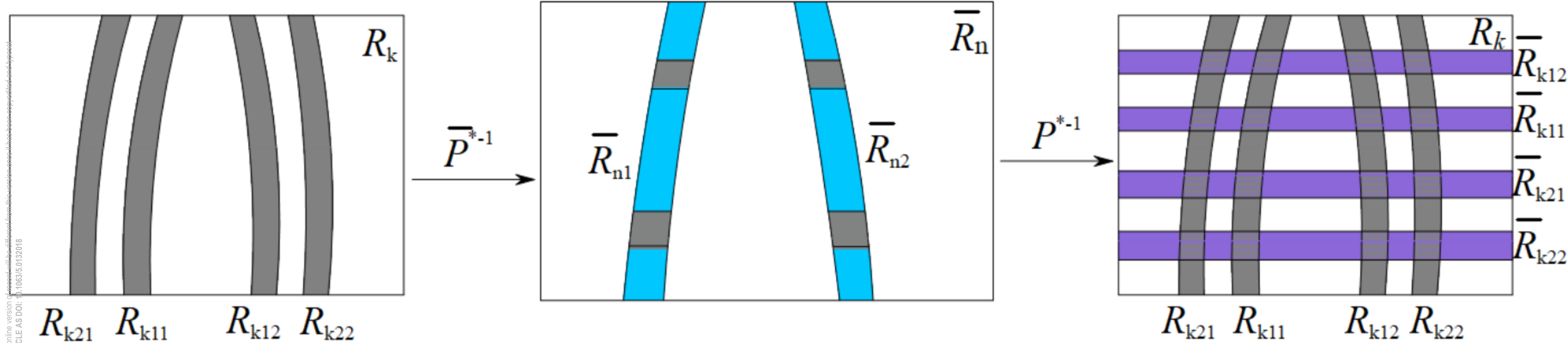


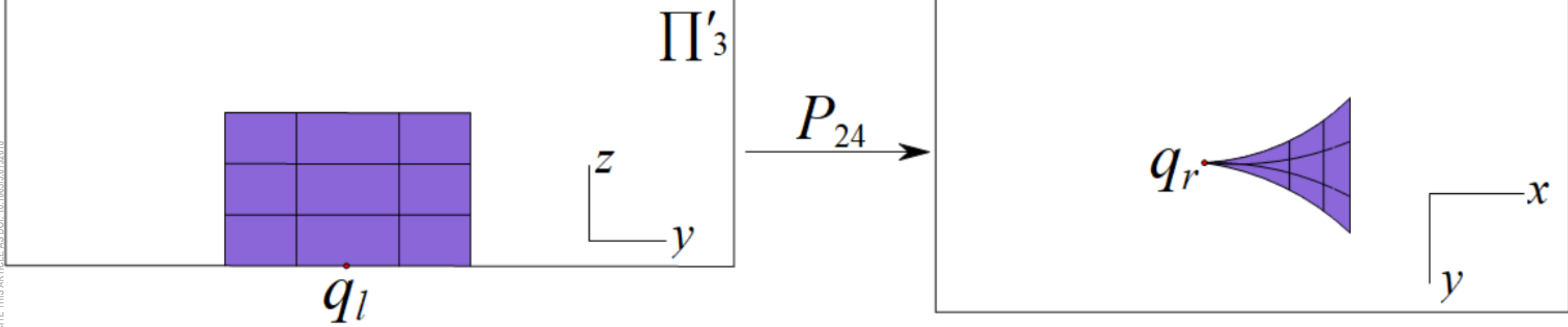
P_{11} →

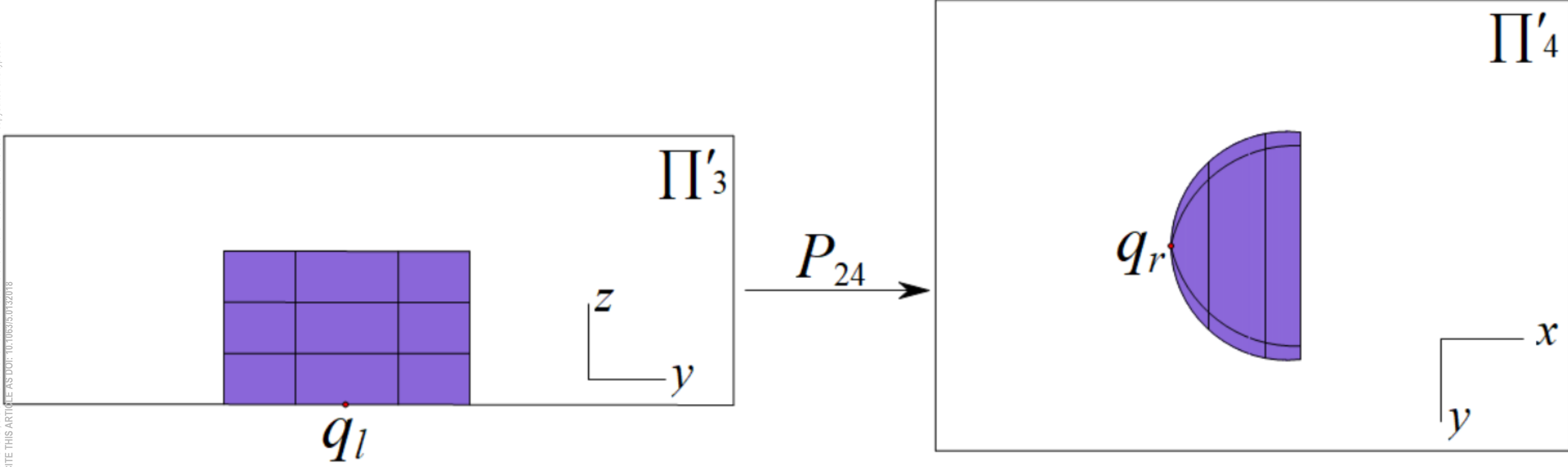








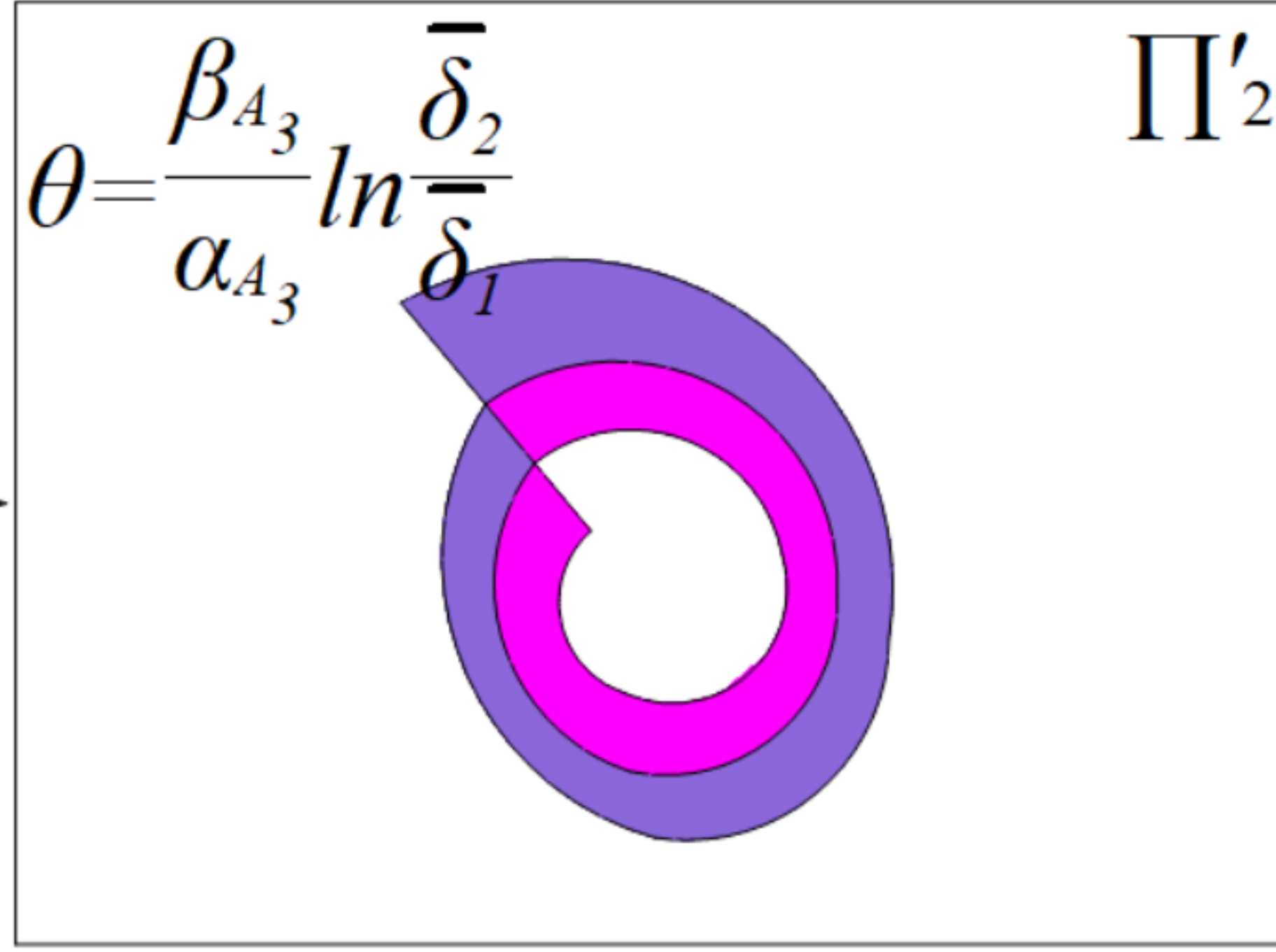


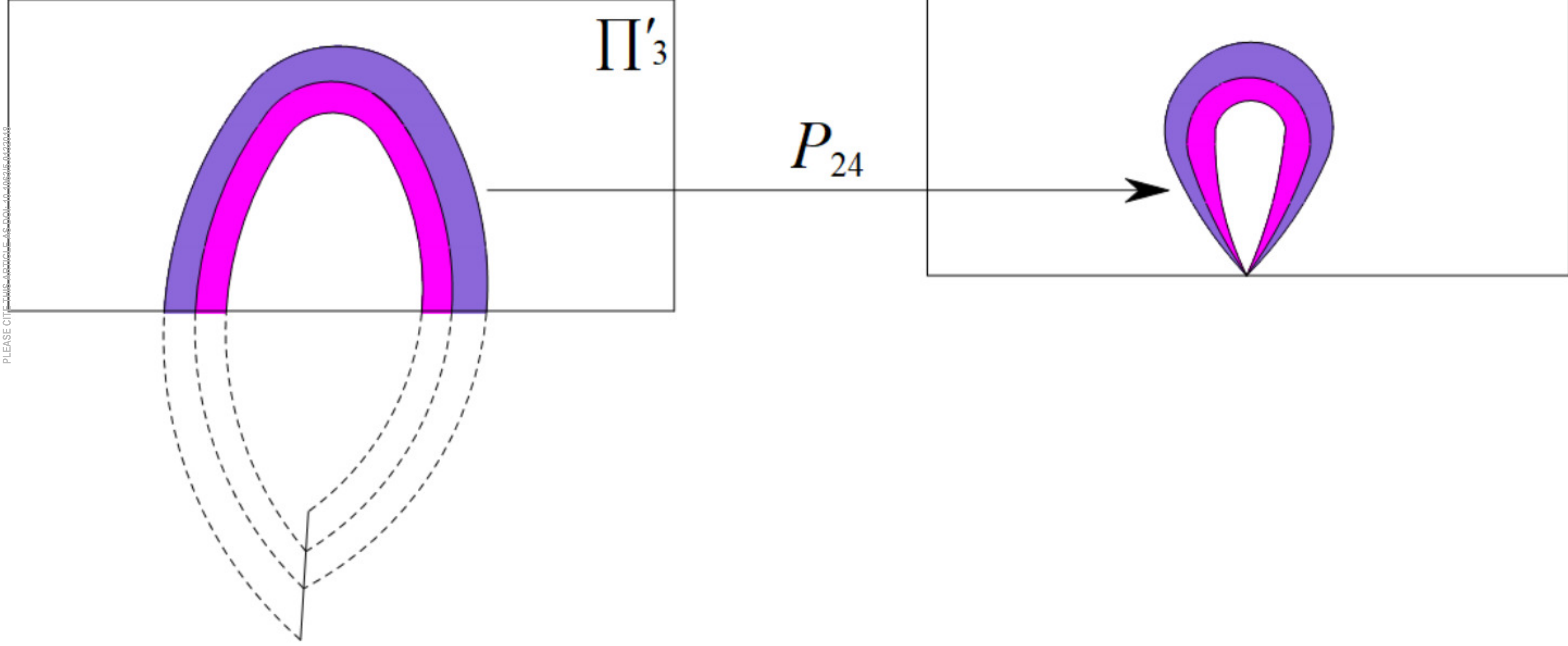


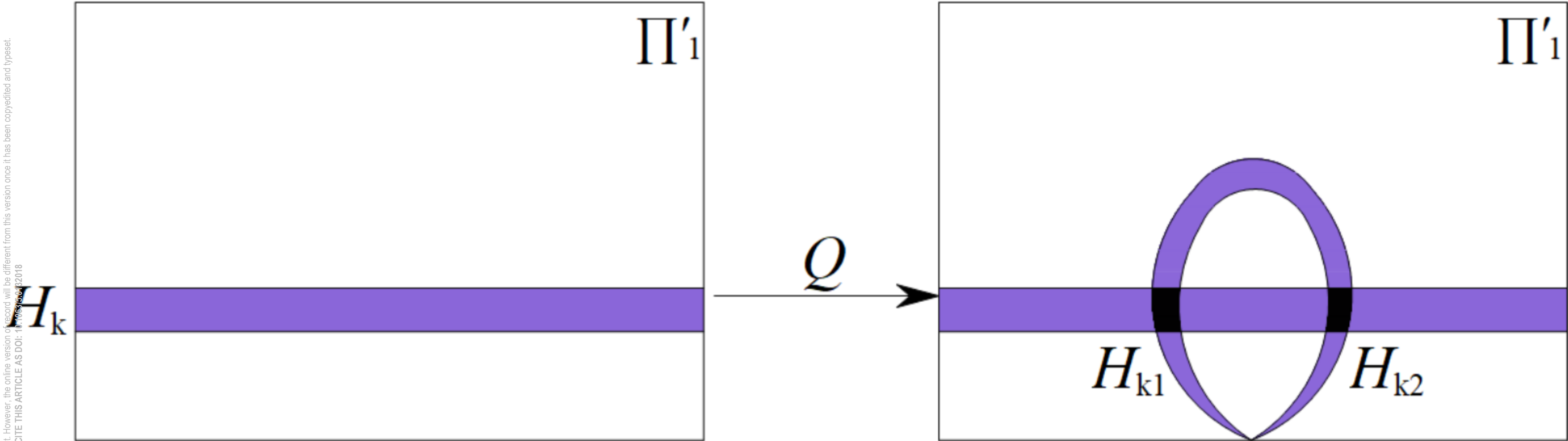
H_k
 H_{k+1}

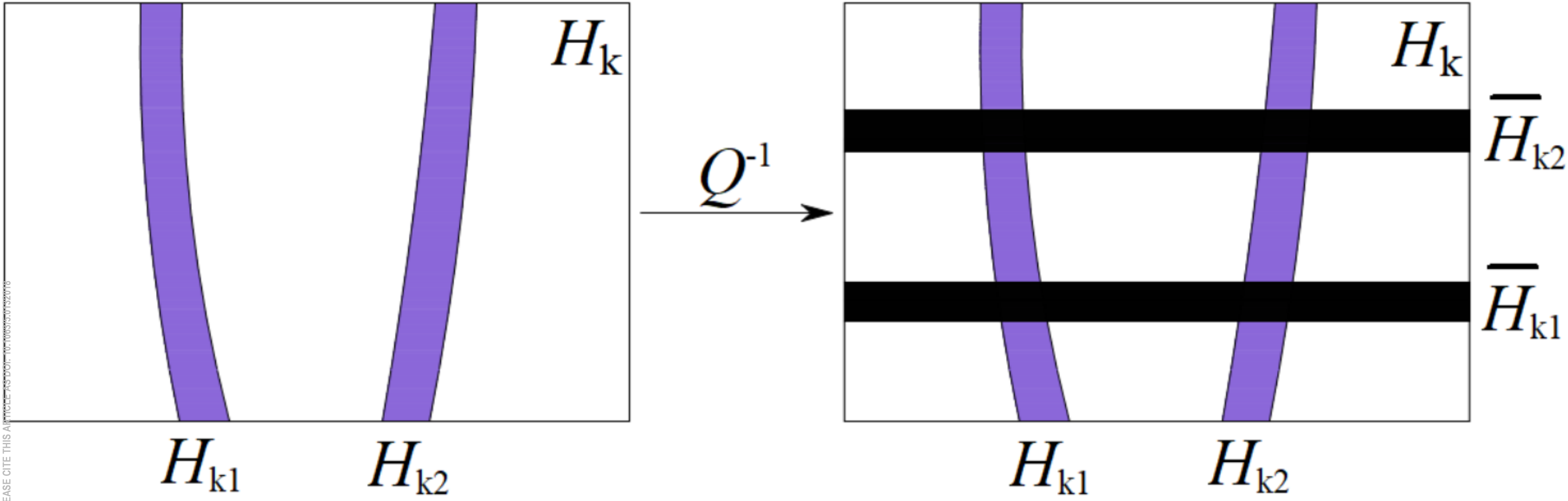


P_{21} →

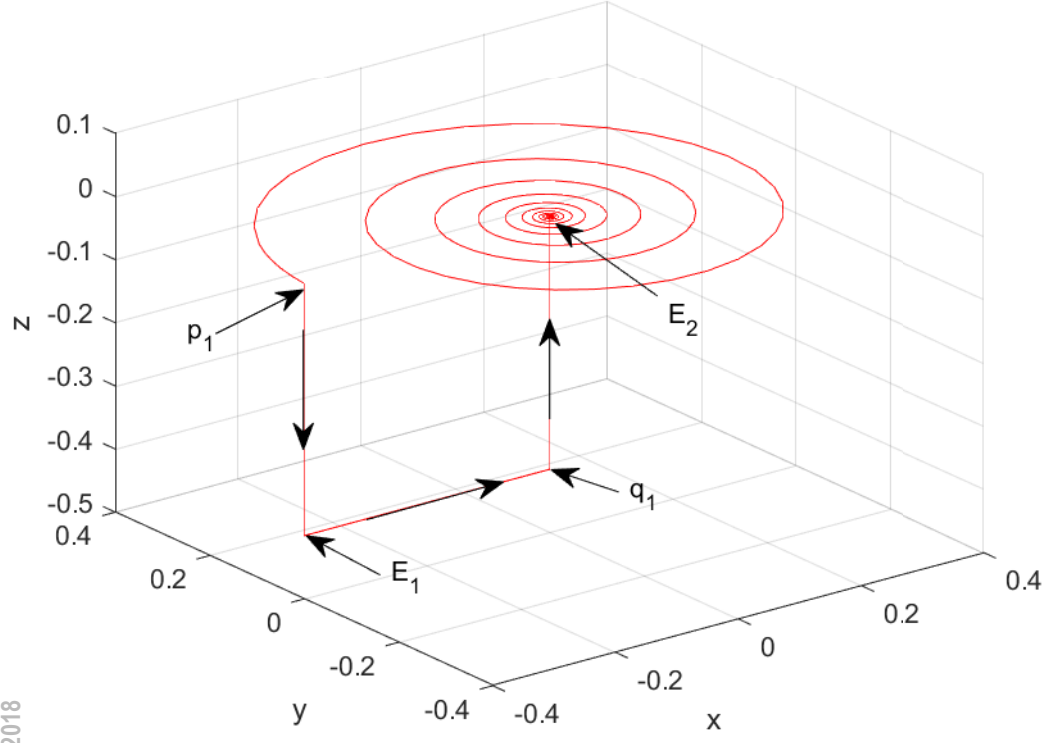




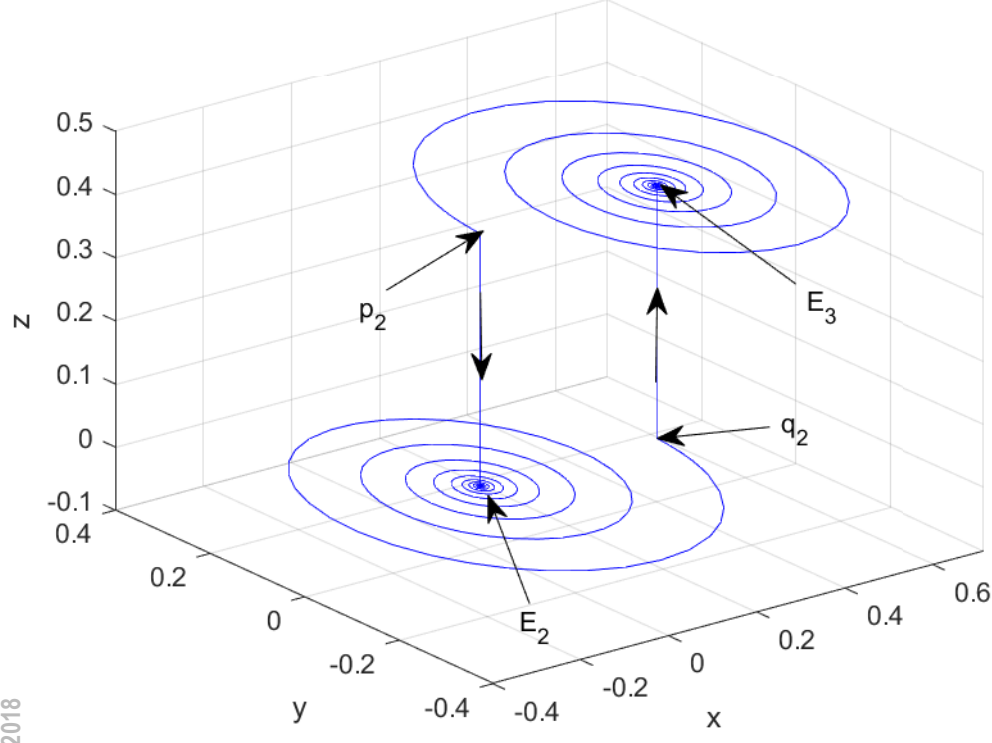




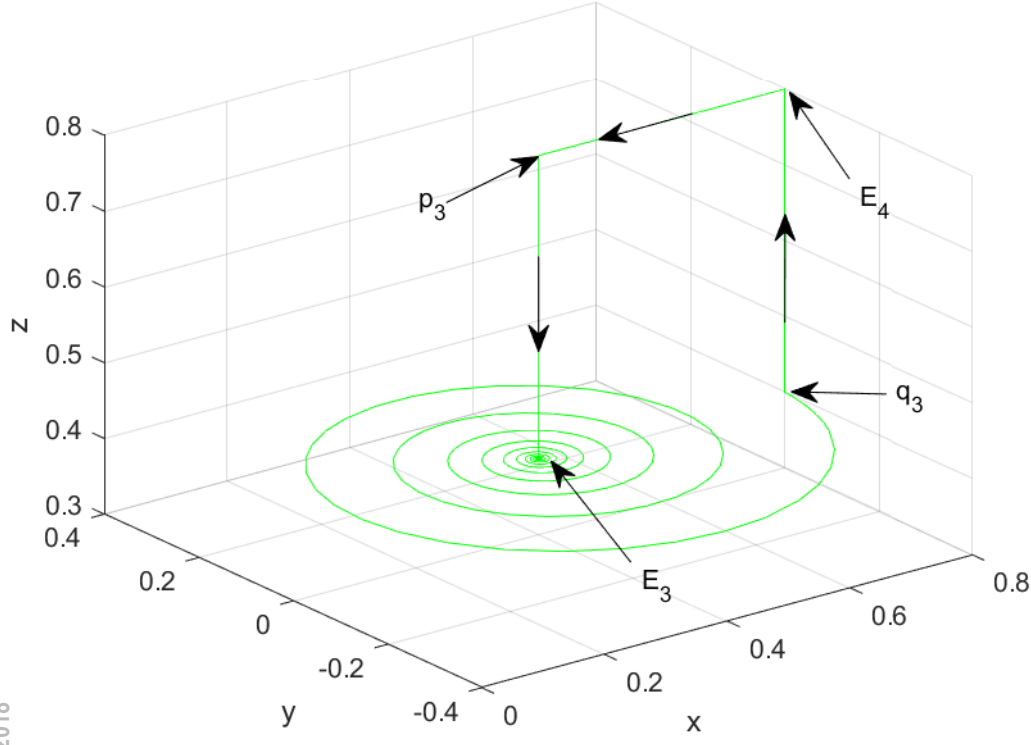
This is the author's peer reviewed, accepted manuscript. However, the online version of record will be different from this version once it has been copyedited and typeset.
PLEASE CITE THIS ARTICLE AS DOI: 10.1063/5.0132018



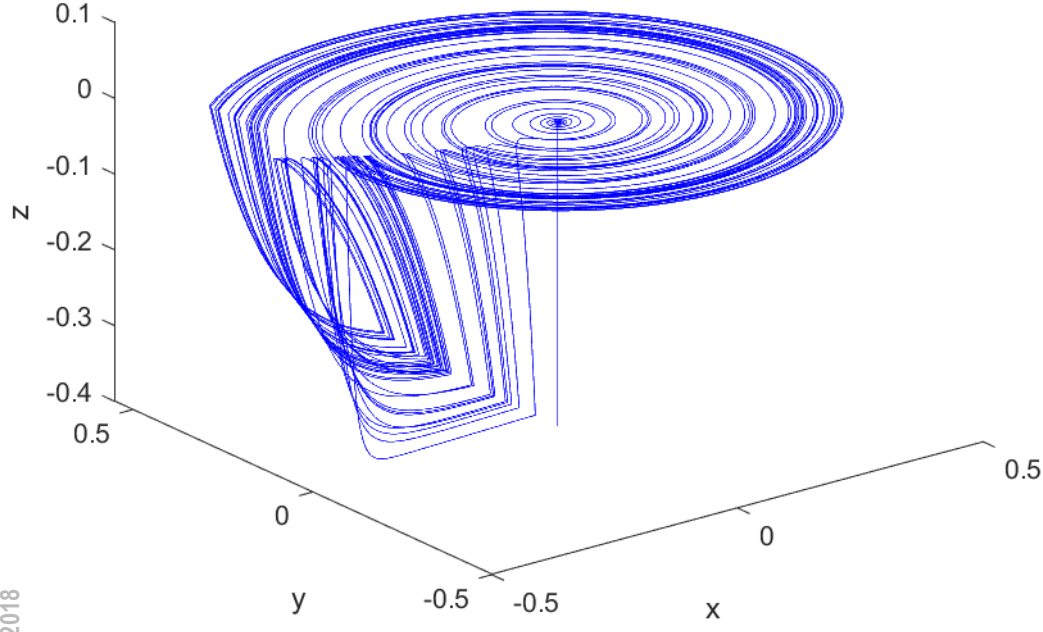
This is the author's peer reviewed, accepted manuscript. However, the online version of record will be different from this version once it has been copyedited and typeset.
PLEASE CITE THIS ARTICLE AS DOI: 10.1063/5.0132018



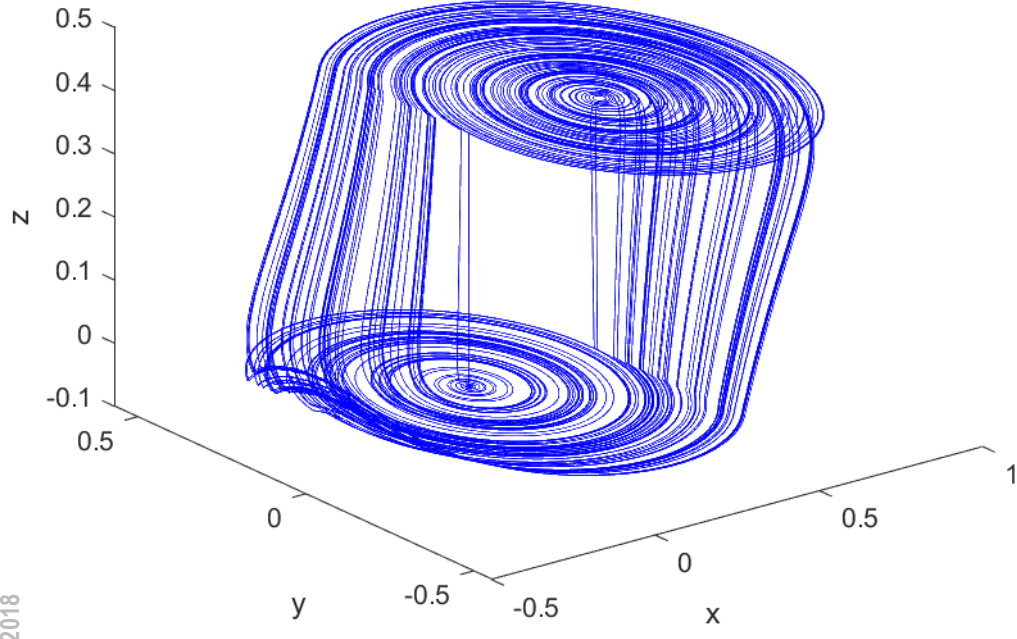
This is the author's peer reviewed, accepted manuscript. However, the online version of record will be different from this version once it has been copyedited and typeset.
PLEASE CITE THIS ARTICLE AS DOI: 10.1063/5.0132018



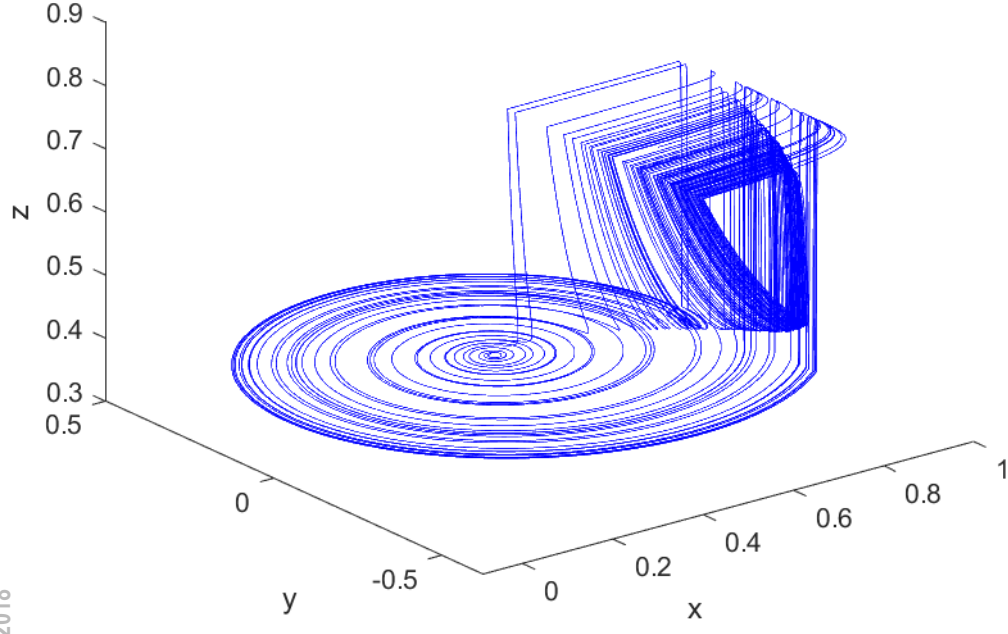
This is the author's peer reviewed, accepted manuscript. However, the online version of record will be different from this version once it has been copyedited and typeset.
PLEASE CITE THIS ARTICLE AS DOI: 10.1063/5.0132018



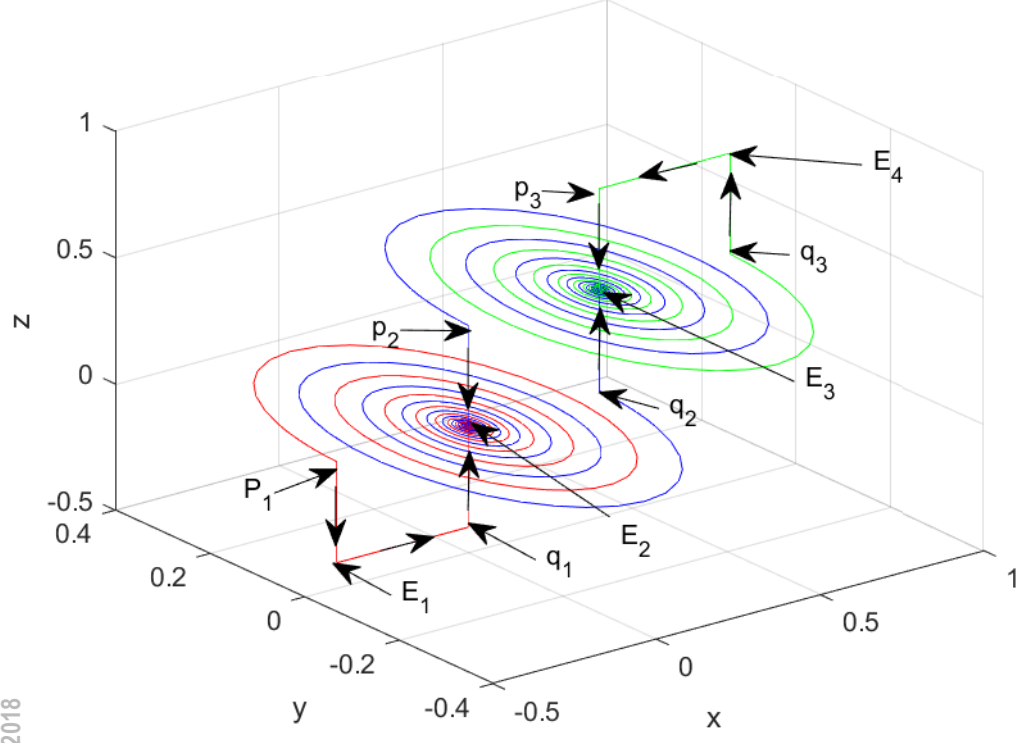
This is the author's peer reviewed, accepted manuscript. However, the online version of record will be different from this version once it has been copyedited and typeset.
PLEASE CITE THIS ARTICLE AS DOI: 10.1063/5.0132018



This is the author's peer reviewed, accepted manuscript. However, the online version of record will be different from this version once it has been copyedited and typeset.
PLEASE CITE THIS ARTICLE AS DOI: 10.1063/5.0132018



This is the author's peer reviewed, accepted manuscript. However, the online version of record will be different from this version once it has been copyedited and typeset.
PLEASE CITE THIS ARTICLE AS DOI: 10.1063/5.0132018



This is the author's peer reviewed, accepted manuscript. However, the online version of record will be different from this version once it has been copyedited and typeset.
PLEASE CITE THIS ARTICLE AS DOI: 10.1063/5.0132018

